# Contemporary, Holocene, and Quaternary deformation of the Asal Rift, Djibouti: Implications for the mechanics of slow spreading ridges

Ross Stein, Pierre Briole, Jean-claude Ruegg, Paul Tapponnier, Francoise Gasse

JOURNAL OF GEOPHYSICAL RESEARCH, VOL. 96, NO. B13, PAGES 21,789–21,806, DECEMBER 10, 1991

# Contemporary, Holocene, and Quaternary Deformation of the Asal Rift, Djibouti: Implications for the Mechanics of Slow Spreading Ridges

ROSS S. STEIN

*U.S. Geological Survey, Menlo Park, California*

PIERRE BRIOLE, JEAN-CLAUDE RUEGG, AND PAUL TAPPONNIER

*Institut de Physique du Globe de Paris, France*

FRANCOISE GASSE

*Laboratoire d'Hydrologie et de Géochimie Isotopique, Université de Paris-Sud, France*

Because the frequency and character of rifting events along mid-ocean ridges are largely unknown, how the repetition of such events gives rise to rift structures is unexplored. The Asal rift in the Afar depression of Djibouti, Africa, provides the world's best subaerial analogue for young slow spreading mid-ocean ridges. Seismic, geodetic, and field observations of a seismovolcanic event in 1978 at Asal yield estimates of the fault and dike locations, geometry, displacement, and volume of basalt extruded in a rifting event. A 6-9 kyr-old lake shore highstand at Asal has been warped downward by 70 m, providing a Holocene measure of the vertical deformation across the rift. The rift topography furnishes an older datum, which we infer to be 34±6 kyr old using the Holocene deformation rate. We find that faults throughout the rift valley are active; Holocene slip rates diminish beyond 4 km from the rift axis; late Quaternary rates decrease beyond 6-7 km. The Holocene slip rates are used to estimate repeat times by taking the displacement on the faults which slipped in 1978 as characteristic; we find tectonic events on individual faults recur every 200-300 years. Half the rift faults slipped together in the 1978 event. If this is typical, then groups of faults are activated every 100-150 years. We suggest that half the events take place in the rift axis accompanied by volcanic extrusion; the remainder occur peripheral to the neovolcanic zone and involve fault slip only, both events having a repeat time of 200-300 years. Given the 10 km width of the rift and its 16 mm $yr^{-1}$ spreading rate, the mean age of the material in the rift should be ~350 kyr, an order of magnitude older than the inferred age of the formation of the rift topography. The subsidence rate of the rift axis during the past 35 kyr is 8-9 mm $yr^{-1}$, with the rate of infilling by volcanic extrusion <1 mm $yr^{-1}$. The resulting net subsidence rate, about equal to the half-spreading rate of the rift, could not be sustained for 300 kyr without significant infilling by lavas. Thus both observations suggest that the long-term vertical deformation in the rift has not been steady state. Instead, we suggest that there is a rifting/filling cycle at Asal, with the most recent filling episode ending ~35 kyr.

## INTRODUCTION

There are but two places where the world ocean rift system comes ashore, Iceland and Djibouti. By virtue of their abnormally high elevation, both sites are anomalous in certain ways: it is widely accepted that Iceland sits atop a hotspot, and seafloor spreading is incipient in Djibouti. Nevertheless, only here are observations of the rift earthquakes, eruptions, morphology, and basalt composition accessible to direct observation. Full spreading rates at Djibouti and Iceland are 17-20 mm $yr^{-1}$. Thus these sites hold promise for a better understanding of the evolution and mechanics of slowly spreading mid-ocean rifts, such as the Mid-Atlantic and Juan de Fuca ridges. Seismovolcanic events at Iceland and Afar share many features, with the distinction that the crust is thicker, tectonic events are deeper, and deformation is consequently broader at Iceland [*Hauksson*, 1983; *Rubin and Pollard*, 1988; *Chen and Morgan*, 1990*a*]. We shall show that the crustal thickness and depth of faulting at the Asal rift in Afar is more typical of mid-ocean ridges, making Asal ideal for investigation.

The Asal rift lies near the western tip of the Gulf of Aden rift (Figure 1*a*), which is propagating westward into the Afar depression through the Gulf of Tadjurah and the Ghoubbet Strait at about 30 mm $yr^{-1}$ [*Courtillot*, 1982; *Courtillot et al.*, 1984; *Acton et al.*, 1991]. The Red Sea rift is also propagating southward toward Asal. About 300 km north of Asal, the Red Sea rift jumps westward into the interior of Afar, creating a broad zone of extensional faulting (Figure 1*b*) [*Barberi and Varet*, 1977]. To the southwest of Asal, the Gaggade and Hanle depressions are aligned parallel to Asal and appear to be sites of distributed deformation which preceded and perhaps now accompanies more intense rifting along the Asal-Ghoubbet and Abhe-Goba'ad spreading axes [*Varet*, 1978; *Gasse*, 1978, 1991; *Tapponnier et al.*, 1990].

The subaerial continuation of the Gulf of Aden rift into the Afar depression displays many of the discontinuities observed along slow spreading mid-ocean ridges (Figure 1*b*), such as overlapping spreading centers, small deviations from axial



Paper numner 91JB02118.
0148-0227/91/91JB-02118$05.00

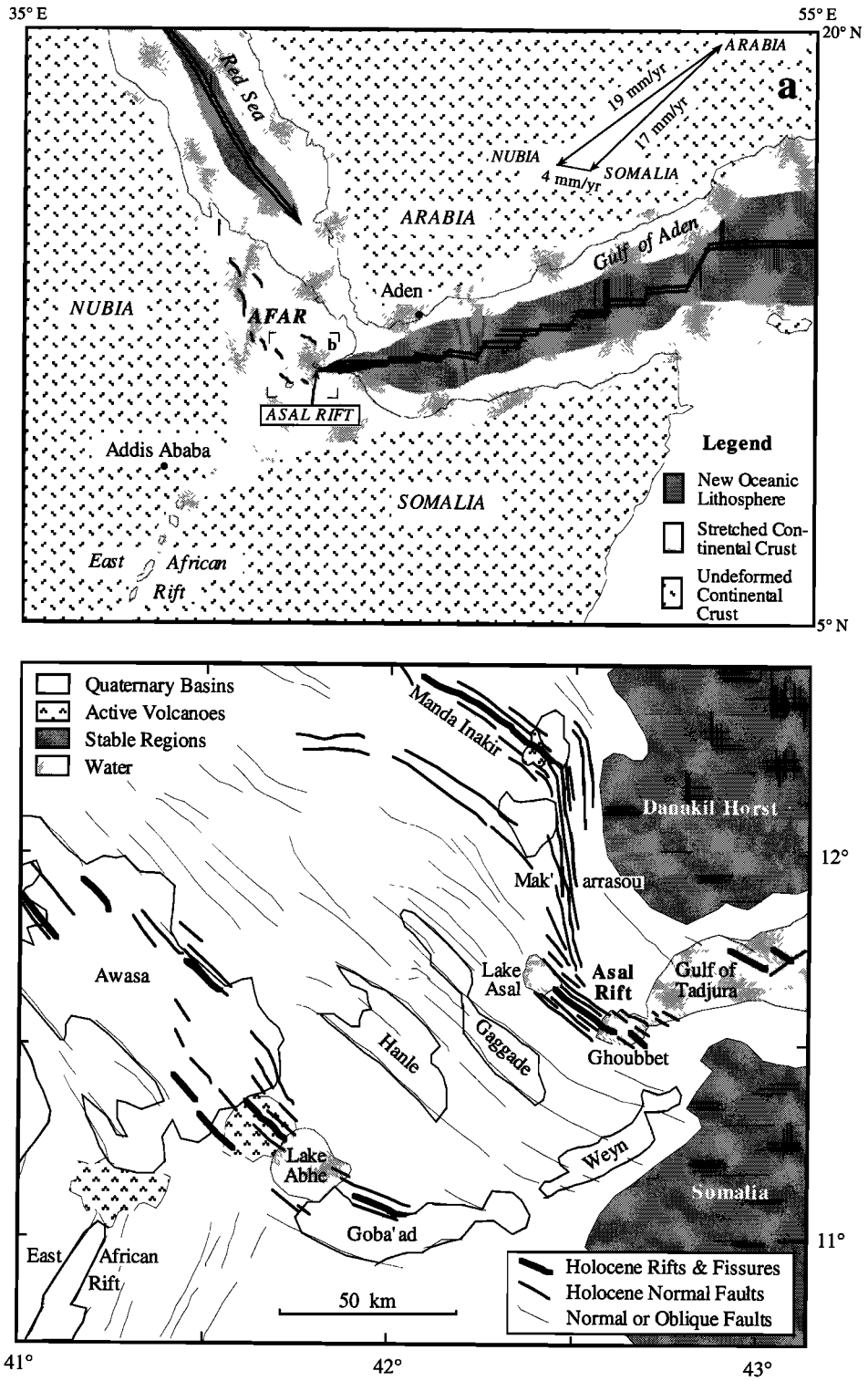


Fig. 1. (*a*) Map showing the propagating Gulf of Aden (Sheba Ridge), Red Sea, and East African rifts [after *Courtillot et al.*, 1987]. Plate motion vectors are inset from *Acton et al.* [1991]. Corners of Fig. 1*b* also shown. (*b*) Localized rifts, volcanism, and distributed extensional faulting in Djibouti [after *Tapponnier et al.*, 1990].

Plate 1. Enhanced Landsat Thematic Mapper image (P166 R52, 21 Feb 85) of the Asal rift zone. Lake Asal is in upper left; Ghoubbet Strait is at lower right. Outside the rift valley, Tadjura Marginal basalts appear bright red and rhyolites within older basalts, such as the Stratoid, are yellow. Within the rift, the 1978 flow is darkest, inner floor basalts appear very dark, lower Axial Series basalts are blue-green to purple, tuffs and hyaloclastites are pink, and Holocene deposits of Lake Asal are light blue-white. Holocene highstand is marked by southeast limit of these deposits across rift. Upper left registration mark is at 11°45'N/42°25'E; lower right is 11°30'N/42°35'E.

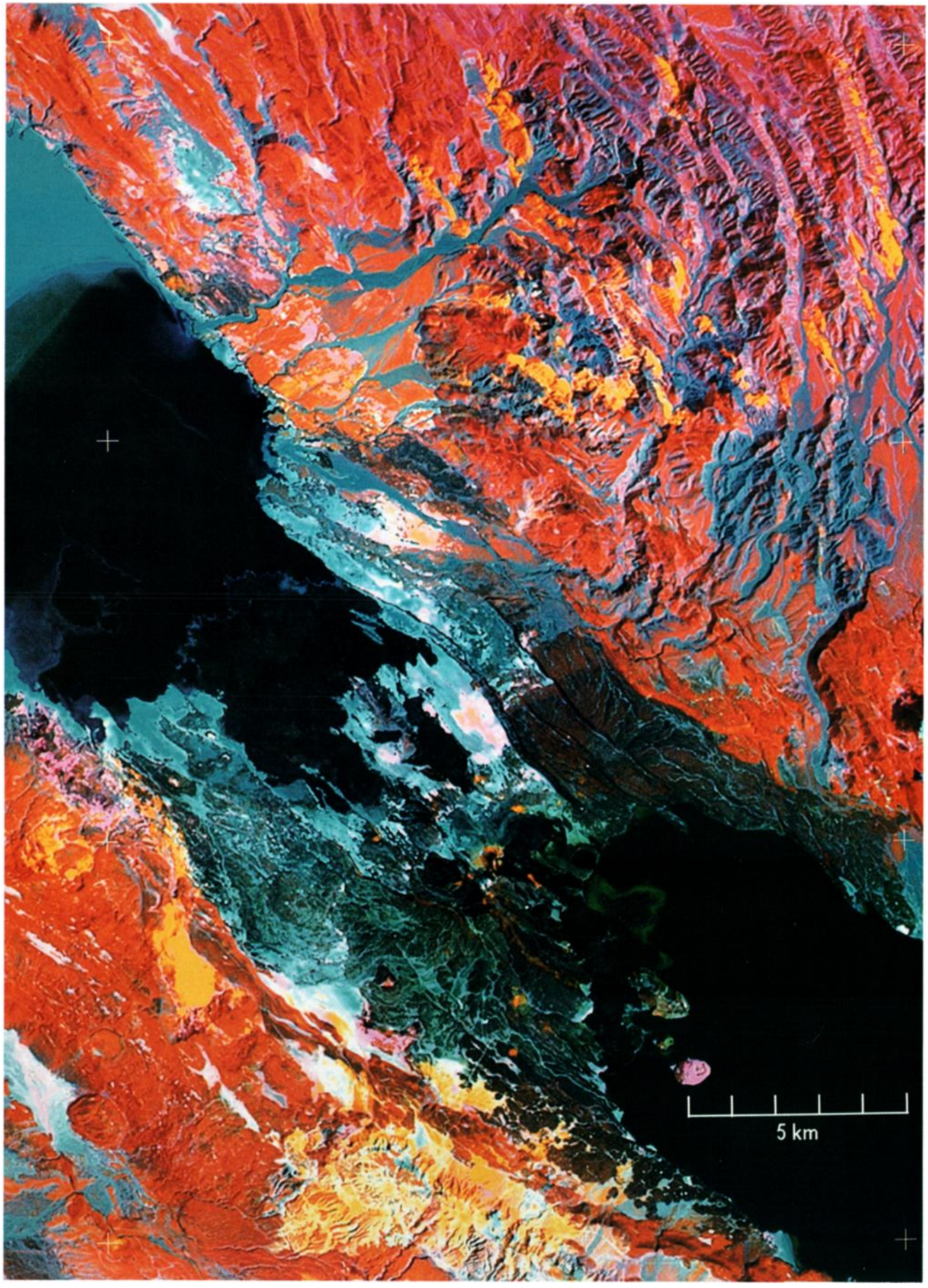
5 km

linearity, nonoverlapping offsets, and sections of oblique spreading [eg., *Tucholke et al.*, 1991; *Phipps Morgan*, 1991]. Some 50 km northwest of Asal, Manda Inakir encompasses several volcanoes along a linear rift valley. Asal sustained an earthquake sequence and eruption in 1978 [*Abdallah et al.*, 1979], and according to local accounts, Manda Inakir was the site of an earthquake and basaltic eruption in 1928-1929 [*Vellutini*, 1990]. Between these volcanic centers lies a 25-km-wide zone of closely spaced faults, the Mak'arrasou (Figure 1*b*), which transforms the Asal spreading center 50 km northeast to Manda Inakir [*Tapponnier and Varet*, 1974; *Tapponnier et al.*, 1990; *Vellutini*, 1990]. A similar pattern of eruptive centers along many slow spreading ridges have been described by *Sempéré and Macdonald* [1987], with symmetrical rift segments alternating with zones of distributed oblique faulting, sinuous bends, and propagating rifts.

The 15-km-long subaerial exposure of the Asal rift lies between the Ghoubbet Strait and Lake Asal (Plate 1). The rift is connected to the submarine Gulf of Tadjura ridge, which itself is a continuation of the Gulf of Aden ridge (Figure 1b). The Asal rift exhibits many of the classic features associated with slow spreading ridges. The rift valley is 11.5 km wide, with an inner rift (also called the rift-in-rift) of 7.5 km width. The rift is 300-800 m deep and has walls lined by steep normal faults with throws of up to 150 m. A 1-to 2-km-wide neovolcanic zone lies along the rift axis, displaying several eruptive centers, young basalt flows, rift-axis fissures, and in many places a central volcanic chain or horst. The Moho lies at a depth of 6-10 km in the Asal-Gulf of Tadjura region, similar to its depth beneath mid-ocean ridges, and about half of its depth elsewhere in Djibouti [*Ruegg*, 1975]. The Axial Series basalts that line the rift valley have an oceanic affinity, with an olivine tholeiite composition typical of mid-ocean rift basalts [*Vellutini*, 1990].

Because of its record of contemporary and Holocene deformation, there are a number of key unresolved questions about the evolution, mechanics, and seismovolcanic activity of mid-ocean rifts that can be answered at Asal. How do rift normal faults form, evolve, and become extinct as they move away from the rift axis? How often do fault-slip and volcanic events occur along a given rift segment? Are these events localized to the rift axis, do events migrate throughout the rift valley, or do they occur outside of the valley? Are the rift deformation and basaltic flux steady state or episodic? And finally, what is the depth of active faulting, or the limit of brittle elastic behavior, on a slow spreading rift? We endeavor to answer these questions at Asal for the insights they may impart on the less accessible mid-ocean rifts.

## DATA

We compare deformation associated with an historical seismovolcanic cycle to the Holocene deformation recorded by the Lake Asal highstand and to the still older deformation preserved by the topography. Thus the principal data considered are leveling and field observations of the 1978 seismovolcanic event, measurements of the age and elevation of the Holocene highstand of lake Asal, and the rift topography.

### *Deformation Associated With the 1978 Seismovolcanic Event*

A seismic swarm began in the rift on 6 November 1978. The largest earthquake ($m_b$=5.3) struck near the rift axis on 7 November 1978 in the northwest end of the Ghoubbet Strait (Figure 2) [*Ruegg et al.*, 1980; *Lépine et al.*, 1980]. The ensuing seismic swarm lasted for 2 months, with most earthquakes occurring along the axial trend of the rift in the Ghoubbet, the activity migrating eastward [*Abdallah et al.*, 1979]. Five to seven inner rift normal faults slipped 0.15-0.5 m over lengths of 4-12 km (Figure 3*a*) [*Abdallah et al.*, 1979; *Le Dain et al.*, 1979]. *Lépine et al.* [1980] obtained a seismic moment $M_o$=1.7 x $10^{17}$ N m (for $\mu$=3 x $10^{10}$ Pa) from conversion of the magnitude of the two largest events. The earthquake was followed by extrusion of 1-2 x $10^7$ $m^3$ of lava through fissures that fed a new eruptive center, Ardoukoba, located in the rift axis 8 km northwest of the main shock [*Allard et al.*, 1979] (Figure 3*a*).

Deformation associated with the 1978 event was measured by geodetic networks [*Ruegg et al.*, 1979, 1984]. A trilateration net of 22 stations was surveyed in 1972/73 [*Institut Géographique National de France*, 1975], and resurveyed following the earthquake in November 1978 and in 1984 (Figure 3*b*, inset). During the 1972-1978 period spanning the earthquake (termed the "coseismic period"), up to 1.9 m of extension was measured, oriented perpendicular to the rift axis [*Ruegg et al.*, 1979]. *Tarantola et al.* [1980, 1979] found that the extension could be explained by 1.5-3.0 m opening of two dikes extending 20 km along the rift axis.

A First order (highest precision) leveling line was also surveyed in 1972 [*Institut Géographique National de France*, 1975], and resurveyed in 1979 and 1984 [*Ruegg and Kasser*, 1987] (Figure 3a). About 0.7 m of inner rift subsidence and 0.2 m of flank uplift was observed during the coseismic period. During the 6 years after the earthquake, 0.15 m of domal uplift was observed within 10 km of the rift axis (Figure 4). Although the geodetic epoch is brief, the combined coseismic (1972-1979) and postseismic (1979-1984) record (Figure 5*a*) furnishes a major part of the eruption-earthquake cycle.

### *Deformation Since the Lake Asal Highstand*

The water level of Lake Asal stood 160 m above sea level at 9-6 kyr, as shown by well-preserved lake shorelines. About 6-5 kyr, the lake level dropped by 310 m [*Gasse*, 1978], and is now 155 m below sea level. The highstand is preserved by former shoreline markers, which fortunately are roughly coincident with the leveling route (Figure 3*a*). In the central Asal rift, 48 $^{14}C$ dates along the highstand were obtained by *Gasse and Fontes* [1989] on inorganic carbonates, mollusc shells, stromatolites (algal mats) and travertines (Figure 3*b*); the mean age is 7.6 kyr, with an average uncertainty of 240 years and a weighted rms variation about the mean of 1.2 kyr (Figure 6 and Table 1). Nearly all fault blocks are sampled in several locations, and the highstand can be identified and correlated across the normal faults between $^{14}C$ sample sites. *Ruegg et al.* [1990] measured the elevation of 104 Lake highstand markers by trigonometric leveling (Figure 3*b*); the typical combined uncertainty of the highstand position and geodetic error is 1 m. Sites included stromatolites, ripple marks, shell layers, and topographic shelves or berms. These points provide an accurate record of the vertical deformation in the rift since 9 kyr (Table 2). Up to 70 m of relative subsidence took place in the rift during the past 9 kyr (Figure 6), yielding a subsidence rate of the rift axis relative to its margins of 8 mm $yr^{-1}$, about the same as the half-spreading rate of the Arabia-Somalia plate motion determined by *Acton et al.*

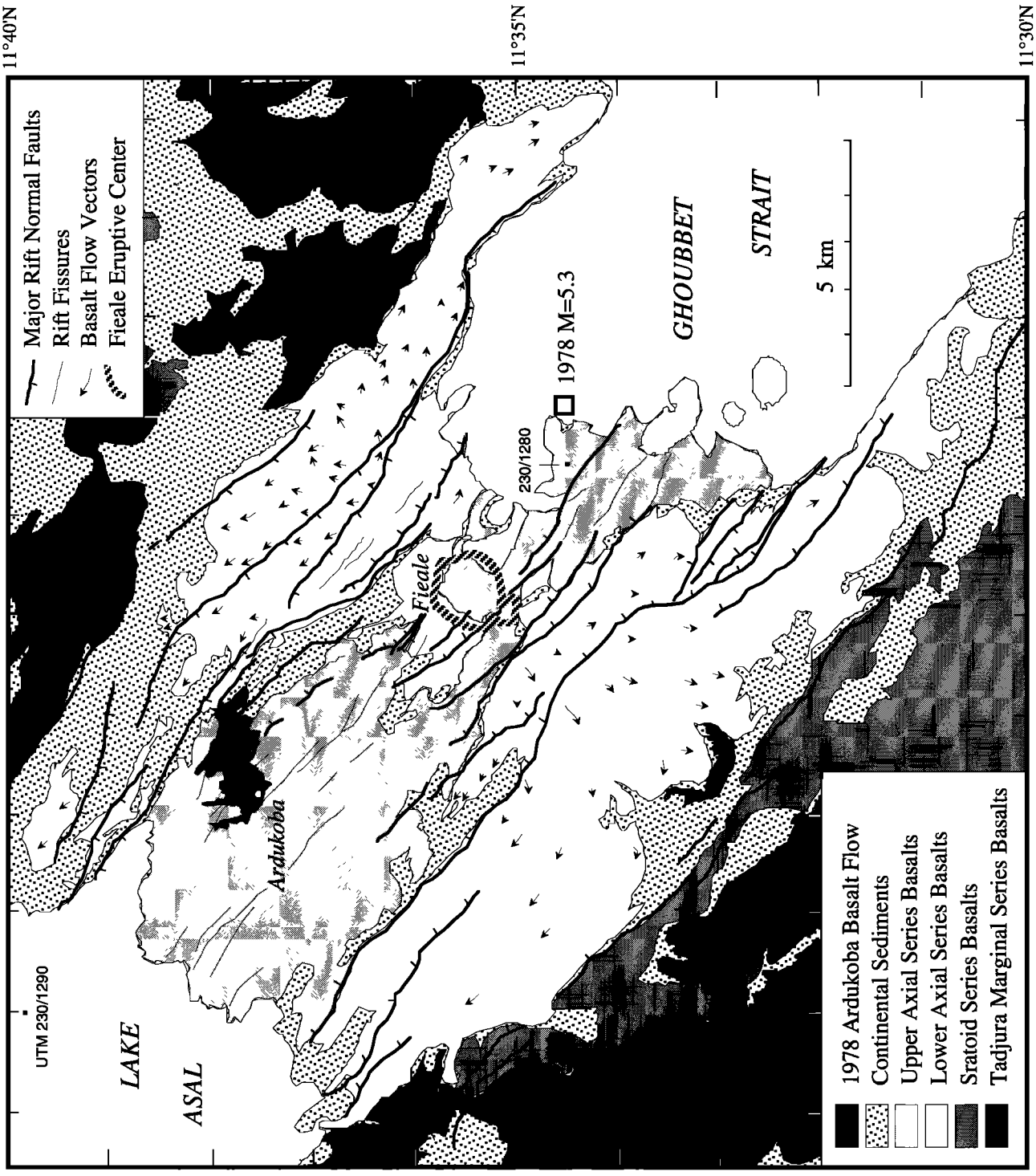


Fig. 2. Geologic map of the Asal rift, simplified from *Stieltjes* [1980], showing the 1978 epicenter and basalt flow, major rift normal faults, fissures, and flow directions for the older Axial Series basalt.

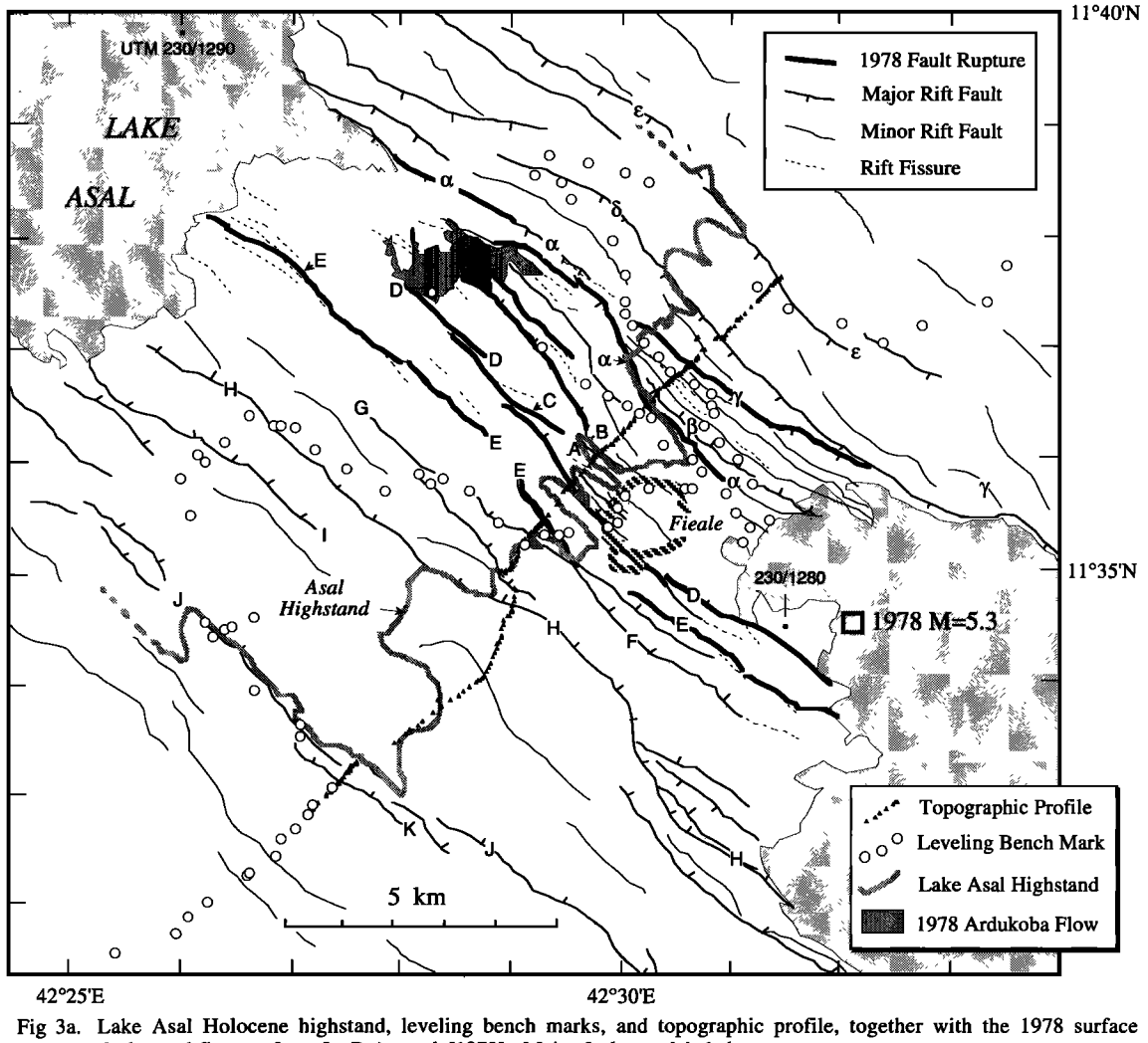


Fig 3a. Lake Asal Holocene highstand, leveling bench marks, and topographic profile, together with the 1978 surface ruptures, faults, and fissures from *Le Dain et al.* [1979]. Major faults are labeled.

[1991]. Since little motion can be resolved between Nubia and Somalia (Figure 1*a*), this vector is nearly the same as the Arabia-Africa motion first precisely determined by *Chase* [1978] and recently confirmed by NUVEL-1, which is 17.6 mm $yr^{-1}$ oriented normal to the rift axis along N50°E [*DeMets et al.*, 1990]. *Gaulier and Huchon* [1991] argue that this spreading direction has been maintained since 1.7-1.2 Ma, although block rotation may alter this age.

Because the rift margins have remained nearly stable with respect to sea level during the past 6 kyr, the relative subsidence rate of 8 mm $yr^{-1}$ is also an absolute subsidence rate. Marine beach deposits within several meters of sea level were dated along the northeast and southwest margins of the Ghoubbet to be 0.5-5.8 kyr old by *Gasse and Fournier* [1983]. These deposits are located southeast of the Asal rift, at about the same distance from the Asal axis as the ends of the Asal highstand shown in Figures 3*b* and 6. Thus the rift axis has been dropping at about 8 mm $yr^{-1}$.

### *Quaternary Deformation Inferred From the Rift Topography*

In 1990, a straight topographic profile located as close as possible to the Lake Asal highstand was surveyed by trigonometric leveling across the rift at ~50 m spacing (Figure 3*a*). Faulting, broadscale warping, and deposition of basalt flows onto the rift floor (Plate 1 and Figure 2) act to create the modern rift topography. The cohesive basalt formations preserve fault morphology better than sedimentary rocks, and in the arid environment of the Afar, rates of erosion are slow (for example, the maximum topographic slope of the faulted fronts is >65°; similar range fronts in the U.S. Basin and Range province slope are 15-30°). Thus the topography is modified more by tectonism than erosion, even where topographic gradients are steep. If the topography was relatively flat before the rift formed, then it can be used as a surrogate structural datum yielding the cumulative deformation that has occurred since the modern rift formed. No ages have been determined for the Axial Series basalt flows (Figure 2). Diatomaceous sediments underlie basalt flows in the inner rift, but these sediments lack datable fossils. The same diatomites species 100 km to the west of Asal have been dated at 25.4-34.4 kyr [*Gasse and Stieltjes*, 1973]. Gasse and Stieltjes infer a similar age for diatomites in the Asal rift and suggest that the basalt flows there postdate ~25 kyr. The age of the Stratoid Series, which extends from the margins of the rift and covers much of the Afar surface outside of the rift zone, ranges from 4.4 to 0.4 Ma [*Varet*, 1978], with most ages near the rift closer to 1-2 Ma [*Courtillot et al.*, 1984]. Near the Asal rift margin, *Richard* [1979] obtained a date of 0.9±0.9 Ma for the Stratoid series basalts.

### *Comparison of the Three Deformation Periods*

The resemblance among the 1972-1984 elevation changes, the Asal highstand deformation, and the topography is evident

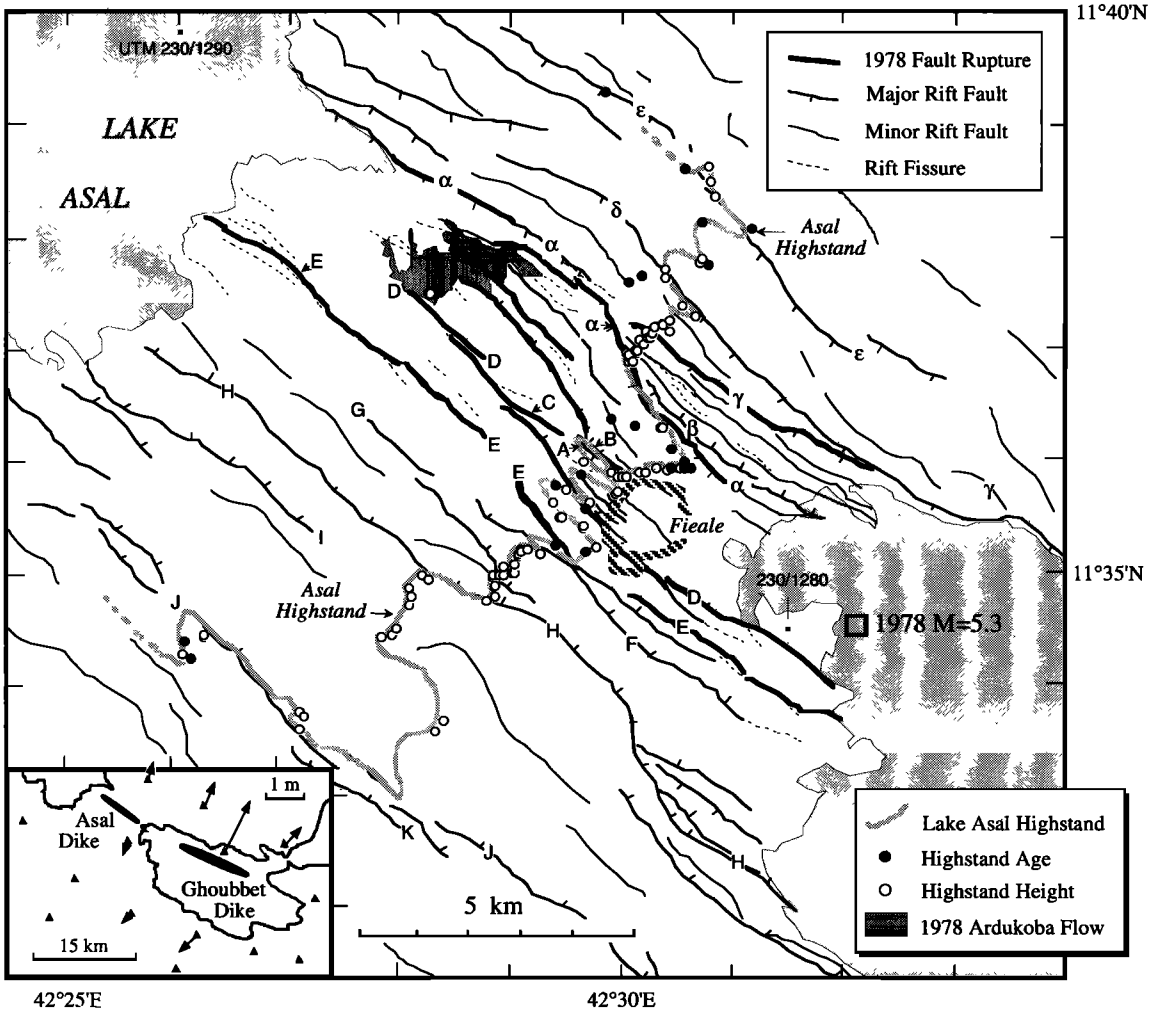


Fig. 3*b*. Lake Asal highstand observations, including radiocarbon dates from *Gasse and Fontes* [1989] and height measurements by *Ruegg et al.* [1990] connected by the inferred shoreline. Trilateration network used by *Tarantola et al.* [1979, 1980] to deduce dike geometry is inset.

in Figure 5: all profiles show pronounced inner rift subsidence associated with slip on the rift normal faults. Both the highstand and topographic profiles are asymmetrical, with a steeper and higher northeast wall. There are also key differences: the long-term deformation revealed in the bottom two panels is broader than that in 1972-1984. Only faults within 2 km of the rift axis ruptured in 1978, whereas faults throughout the rift have been active during the two older intervals. Because the cumulative fault slip varies along strike of the faults, the comparison between the Highstand and topographic profiles is most direct when the topographic and lake highstand profiles intersect. At the southwest end, the similarity is less compelling, but there the topographic profile is located 1-2 km from the Lake highstand (see Figure 3*a*).

## ANALYSIS

### *Geometry and Moment of the 1978 Event*

The 1978 seismovolcanic event permits us to infer the geometry and displacement of the reactivated inner rift faults crossed by the leveling route. Broadscale coseismic (1973-1978/79) horizontal distance changes across a trilat-eration network were interpreted by *Tarantola et al.* [1979, 1980] to result from dilation of two subsurface dikes in the Asal rift and Ghoubbet Strait (Figure 3*b*, inset). Evidence for dike inflation also comes from field observation of many closely spaced surface fissures along the rift axis by *Le Dain et al.* [1979] (Figure 2) and from the Ardukoba eruption at the northwest end of the rift. Because of the large interstation spacing, the trilateration network is insensitive to normal faulting near the rift axis. Thus we first remove the vertical deformation associated with dilation of the two dikes from the leveling data, and then interpret the residual elevation change by normal fault slip (Figure 4*a*).

We match the residual 1972-1979 elevation changes across the rift to the vertical deformation produced by slip on a series of rectangular dislocations, following *Okada* [1985]. The upper edge of the faults were set at the free surface, and the length and approximate location of faults α, β, γ, E+F, and C+D are fixed using field observations [*Le Dain et al.*, 1979]. Since *Le Dain et al.* [1979] saw no clear evidence for strike-slip motion, and because the leveling data are insensitive to the strike-slip component, we restrict the models to pure dip slip.

The close proximity of the normal faults limits the extent to which differences in their geometry can be inferred. Thus we performed a set of trials in which all faults dipped 45°, 60°, 75°, and 85°. The residuals on the upthrown (outer) blocks of the normal faults were minimized when the dips were 60-80°, and when the outer faults reached a lower depth of about 3 km; the mean residual per bench mark is 74 mm. The best solution is

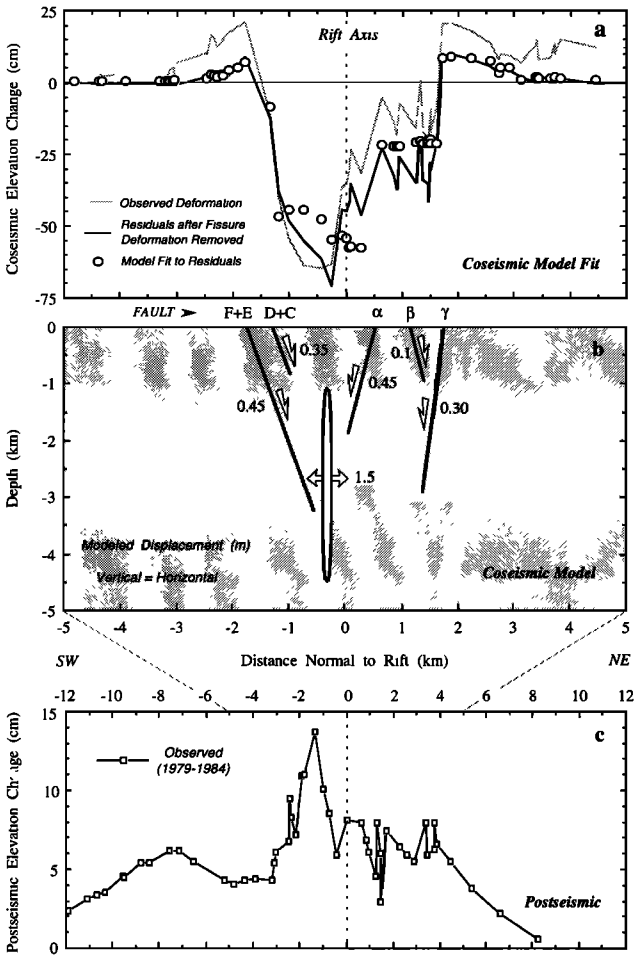


Fig. 4. (*a*) Profile of observed and predicted rift deformation along leveling route shown in Figure 3*a* projected along N36°E. (*b*) Cross section of the dislocation model which produces the predicted elevation changes in Figure 4*a*. (*c*) Postseismic elevation changes; note change in scale.

shown in Figure 4, and the parameters for both the dikes and faults are listed in Table 3. The 1979-1980 epicenters clustered near faults α, β, and γ [*Ruegg et al.*, 1982], and although the seismic network was too sparse until 1986 for reliable depth determination, since then depths have been <4 km [*Lépine et al.*, 1980]. The surface displacement for faults α, β, and γ, and C+D [*Abdallah et al.*, 1979; *Le Dain et al.*, 1979] is similar to the mean slip at depth inferred from the inversion (compare the second and third columns in Table 4). The average surface slip on these faults is 0.30 m; the mean inferred slip at depth is 0.33±0.16 m.

Comparison of the moment estimated from the geodetic deformation to the seismic moment of the earthquakes estimated from the waveforms reveals that aseismic deformation dominated in the 1978 event. The geodetically determined moment, where $M_o=\mu\Sigma uA$ ($u$ is the slip and $A$ the fault area), is 6 x $10^{17}$ N m (Table 3). This is a lower bound, because fault slip extended into Ghoubbet toward the mainshock epicenter, and because fissure opening and dike inflation accompanied the faulting. The contribution of the fissure opening and dike inflation to the geodetic moment can be included by using the inversion of the horizontal geodetic data of *Tarantola et al.* [1980]. The moment associated with faulting and fissuring then becomes 22 x $10^{17}$ N m (Table 3). We use 1.1 x $10^{10}$ Pa as the modulus, μ; this is about 1/3 of modulus of the continental crust, more appropriate for the thin, hot, and attenuating lithosphere [*Morton and Black*, 1975; *Pham Van Ngoc et al.*, 1980] of the rift zone.

The summed seismic moment for the two largest shocks ($m_b$=5.3, 5.0) is 1.7 x $10^{17}$ N m [*Lépine et al.*, 1980]. The summed moment of all other aftershocks is negligible in comparison to the two $m_b$>5 shocks, as the moment of a $M$=5 earthquake is 30 times that of a $M$=4 shock. Thus, little of the deformation associated with the 1978 seismovolcanic episode was released at seismic frequencies. Instead, the earthquakes may have triggered fault slip or accompanied dike intrusion and the Ardoukoba eruption. *Solomon et al.* [1988] found that the global rate of seismic moment release along slow spreading mid-ocean ridges is confined to the inner floor of the rift valley and accounts for no more than 10-20% of the rate of plate separation across the rift valley, in accord with these results. *Chadwick et al.* [1991] found evidence for basaltic extrusion sometime during 1981-1987 along a 15-km-long segment of the southern Juan de Fuca Ridge, which was unaccompanied by earthquakes of $m_b$>4. Both of these findings for slow spreading ridges are compatible with the 1978 event on the Asal rift, in which all of the faulting and intrusion occurred within 2 km of the rift axis, and perhaps 10% of the moment was released seismically (Table 3).

### *Age of Modern Rift Formation*

The profile of the Asal highstand elevation is most like the topographic profile when the highstand elevation is scaled by a factor of 3.75±0.25 relative to the topographic elevation (Figure 7). Given formation of the earliest highstand at 9±1 kyr and assuming a constant rate of deformation, the topography formed since 34±6 kyr. All faults within the 7.5-km-wide inner rift are seen to be active during both time intervals.

The 30-40-kyr period represented by the topography is only a brief increment in the Arabia-Somalia plate breakup. The westward propagating Gulf of Aden spreading center (Figure 1) reached the eastern Afar ~2 Ma, with the Asal-Ghoubbet rift forming about 1.6 Ma [*Courtillot*, 1982]. We interpret the topographic age to mean that sometime before 35 kyr, the rate of rift in-filling by volcanism exceeded the rate of graben formation by faulting and broadscale deformation, so that the structural trough created by the rift was filled by lavas. Since 35 kyr, the rate of extrusion has slowed relative to the rate of faulting and downwarping, creating the modern 300-m-deep rift.

### *Separation of Fault Displacement From Broadscale Deformation*

The Holocene and late Quaternary profiles are produced by fault slip and dike emplacement in the brittle crust that cause short-wavelength deformation [*Rubin and Pollard*, 1988], and also by deeper processes that give rise to longer wavelength deformation, such as isostatic adjustment [*Vening Meinesz*, 1950], lithospheric necking [*Tapponnier and Francheteau*, 1978; *Lin and Parmentier*, 1989, 1990], and elastic or asthenospheric rebound [*Tarantola et al.*, 1979, 1980]. Whereas faulting and fracturing scale with the depth to the center of the sources, which here is about 2 km, the other processes act at greater depth or are governed by the flexural

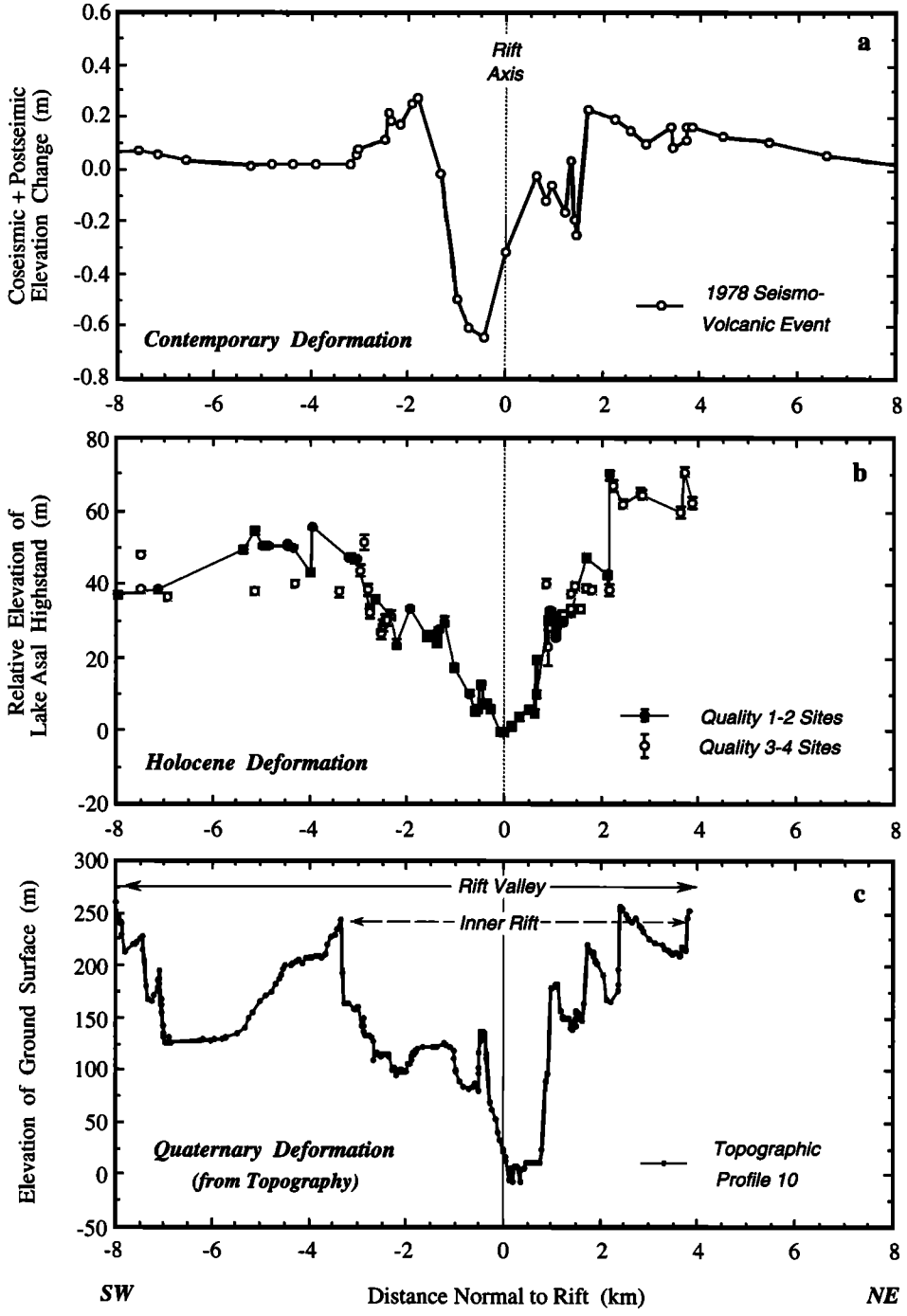


Fig. 5. (*a*) Coseismic+postseismic elevation change, (*b*) elevation of the Lake Asal highstand, and (*c*) elevation of the topography, projected normal to the rift axis.

rigidity of the crust, which scales with the cube of the effective elastic thickness.

To make reliable estimates of the fault throw, we seek to isolate the local faulting and fissuring from the deeper, longer-wavelength processes. The similarity of the 7.6±1.2 kyr and 34±6 kyr deformation profiles (Figure 7) suggests that the same long-wavelength processes occur during both intervals. To represent the long-wavelength deformation, we sought a curve that captures the gross shape of the rift and its limbs. We chose to fit a polynomial of seventh order to the combined highstand and topographic points of Figure 7, in which each data profile received equal weight. Selection of the curve is arbitrary; polynomials of lower order did not yield minima at the rift axis.

To represent the effects of local faulting, we use the vertical throw or offset across each fault by extrapolating the elevation difference of points to both sides of each fault from the residuals to the polynomial. The topographic profile and the polynomial are shown in Figure 8*a*; the residuals are shown in Figure 8*b*. The corresponding figures for the highstand profile are Figures 9*a* and 9*b*. Removal of the polynomial would not be necessary for closely spaced observations, such as those

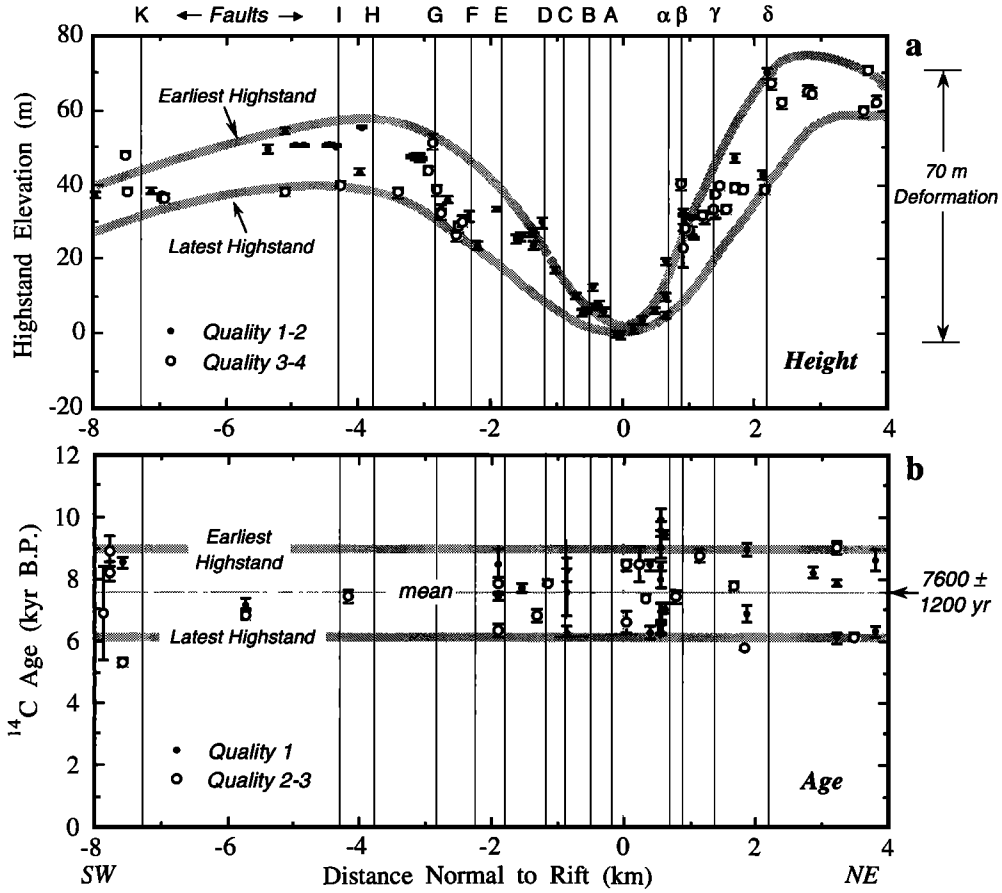


Fig. 6. Profiles of (*a*) elevation of Asal highstand markers measured by *Ruegg et al.* [1990], and (*b*) radiocarbon ages of highstand markers from *Gasse and Fontes* [1989]. Faults (labeled at top) are indicated by vertical lines. The mean age is 7.6 kyr, with earliest highstand at 9 kyr and latest at 6 kyr. Lake level was fixed at 0 km by lake outlet, so deformation during 9-6 kyr is recorded at margins. Site quality is explained in Tables 1 and 2.

along much of the topographic profile. Since the highstand observations are more sparse, however, the offset measured on points far from each fault includes some broadscale deformation or block tilting, which would result in an overestimate of the throw if the polynomial were not used.

The curve drawn through the residuals represents our judgement of a surface that was continuous and flat, or nearly so, at 34±6 kyr in Figure 8*b* and 7.6±1.2 kyr in Figure 9*b*. The fault offset is underestimated by the topography where basalt flows, talus slopes, or alluvial fans have buried the base of the escarpment, such as at faults α, ε, I, and J, so in these cases the surface is extrapolated beneath the cover (Figure 8*b*). The ±1.2-kyr scatter in the age of the highstand, the variable site quality, and the coarser sampling make the extrapolation of the fault offsets for the highstand profile less precise. While the vertical offset for faults α, β, γ, δ, A, and F are clear, for example, offsets for faults E and K are indistinct. Here we were guided by the higher quality sites where possible (Figure 9*b*). The fault offsets are more precise for the topographic profile than for the highstand, but the period of faulting is known for the highstand and only inferred for the topographic profile. Thus the fault slip rates deduced for both epochs have similar uncertainties (see Table 4).

*Holocene and Late Quaternary Fault Slip*

The distribution of slip among the inner rift faults (I-δ) are comparable during the Holocene and late Quaternary intervals (Figure 10). Quaternary faults more than 4-7 km from the rift axis (ε, J, K, and L), however, appeared to have slowed or ceased during the past 8 kyr. It should be noted that the Holocene and Quaternary rates are not fully independent: the late Quaternary slip includes the Holocene component, and the Quaternary rates depend on our estimate of the 35-kyr duration of faulting. There is also an asymmetric distribution of Holocene slip in the rift. The summed slip rate on the northeast wall is 8.1 mm yr$^{-1}$; on the southwest wall it is 5.7 mm yr$^{-1}$ (rates summed for faults A-L (*SW*) and faults α-ε (*NE*) in Table 4). In addition, the northeast wall exhibits greater rates on fewer faults than the southwest wall.

Estimates of the age of each fault can be made if we assume that the faults have slipped at their Holocene rates since inception. Thus, from the cumulative slip on each fault (Figure 11*a*), fault ages can be inferred (Figure 11*b*). If faults formed at the ridge and continued to slip as they are carried away from the rift with time, then in both plots values should increase with distance from the rift. The absence of such a trend suggests that the faults formed at roughly the same time, or that basalt deposition erased the preexisting topography at one time. The mean fault age thus deduced, or alternatively, the age when the basalts were deposited, is 35±22 kyr, in accord with our other estimate of the age of the broadscale rift topography, but with larger uncertainty.

*Tectonic and Volcanic Repeat Times*

*Repeat times for fault slip events.* To convert slip rates to repeat times, we need to know the slip per event. Several well-preserved surface scarps along fault γ show evidence of two to three previous slip episodes with comparable amount of slip.

TABLE 1. Lake Asal Highstand Age Determinations

| Site | UTM-X, km | UTM-Y, km | Distance Along N36°E, km | $^{14}C$ Age, years B.P. | S.D., years | Quality* |
|---|---|---|---|---|---|---|
| 1 | 228.1 | 1283.0 | 0.572 | 9930 | 320 | 1 |
| 2 | 228.1 | 1283.0 | 0.572 | 9590 | 240 | 1 |
| 3 | 228.4 | 1282.7 | 0.638 | 9440 | 160 | 1 |
| 5 | 228.3 | 1282.7 | 0.558 | 9045 | 345 | 1 |
| 6 | 227.0 | 1289.0 | 3.209 | 9045 | 200 | 2 |
| 8 | 227.0 | 1289.0 | 3.209 | 9000 | 200 | 2 |
| 9 | 227.6 | 1285.9 | 1.872 | 8965 | 240 | 1 |
| 10 | 220.1 | 1279.8 | -7.781 | 8900 | 460 | 3 |
| 12 | 223.8 | 1289.9 | 1.149 | 8760 | 200 | 2 |
| G18 | 229.4 | 1286.7 | 3.799 | 8630 | 320 | 1 |
| 20 | 216.7 | 1284.8 | -7.593 | 8540 | 180 | 1 |
| 21 | 225.0 | 1286.7 | 0.239 | 8470 | 570 | 2 |
| 22 | 227.1 | 1283.5 | 0.057 | 8460 | 160 | 2 |
| 23 | 228.1 | 1282.7 | 0.396 | 8460 | 180 | 1 |
| 24 | 226.2 | 1281.4 | -1.906 | 8450 | 540 | 1 |
| 25 | 228.1 | 1283.0 | 0.572 | 8400 | 140 | 1 |
| 26 | 226.6 | 1282.6 | -0.877 | 8300 | 385 | 1 |
| 27 | 228.7 | 1286.1 | 2.880 | 8225 | 160 | 1 |
| 28 | 220.1 | 1279.8 | -7.781 | 8215 | 315 | 3 |
| 30 | 228.3 | 1282.7 | 0.558 | 8010 | 270 | 1 |
| 32 | 228.6 | 1286.8 | 3.210 | 7890 | 120 | 1 |
| 34 | 226.7 | 1282.0 | -1.148 | 7880 | 110 | 3 |
| 35 | 226.2 | 1281.4 | -1.906 | 7860 | 240 | 2 |
| 36 | 227.4 | 1285.8 | 1.652 | 7810 | 150 | 2 |
| 37 | 226.7 | 1281.3 | -1.560 | 7750 | 130 | 1 |
| 39 | 226.6 | 1282.6 | -0.877 | 7580 | 750 | 1 |
| 42 | 220.6 | 1293.7 | 0.794 | 7460 | 200 | 3 |
| 43 | 221.0 | 1284.7 | -4.173 | 7430 | 200 | 3 |
| 44a | 226.2 | 1281.4 | -1.906 | 7420 | 80 | 1 |
| 45 | 227.5 | 1283.4 | 0.322 | 7400 | 110 | 2 |
| 46a | 221.2 | 1281.8 | -5.716 | 7200 | 200 | 1 |
| 47 | 228.3 | 1282.8 | 0.616 | 7060 | 160 | 1 |
| 48 | 228.3 | 1282.7 | 0.558 | 6970 | 260 | 1 |
| 50 | 220.2 | 1279.5 | -7.876 | 6910 | 1500 | 2 |
| 51 | 227.6 | 1285.9 | 1.872 | 6890 | 270 | 1 |
| 54 | 226.2 | 1282.4 | -1.318 | 6820 | 180 | 2 |
| 55 | 221.2 | 1281.8 | -5.716 | 6800 | 140 | 2 |
| 58a | 227.1 | 1283.5 | 0.057 | 6620 | 320 | 3 |
| 60 | 228.3 | 1282.7 | 0.558 | 6460 | 170 | 1 |
| 61 | 228.3 | 1282.7 | 0.558 | 6360 | 185 | 1 |
| 62a | 226.2 | 1281.4 | -1.906 | 6350 | 180 | 2 |
| 65 | 229.4 | 1286.7 | 3.799 | 6320 | 175 | 1 |
| 66 | 226.6 | 1282.6 | -0.877 | 6295 | 190 | 1 |
| 67 | 228.1 | 1282.7 | 0.396 | 6280 | 180 | 1 |
| 69 | 228.3 | 1287.7 | 3.496 | 6170 | 130 | 2 |
| 70 | 228.6 | 1286.8 | 3.210 | 6135 | 170 | 1 |
| 71 | 220.0 | 1282.5 | -6.275 | 5945 | 100 | 2 |
| 72 | 227.2 | 1286.4 | 1.842 | 5760 | 55 | 2 |

*Data from *Gasse and Fontes* [1989]. Quality 1, algal stromatolites or littoral molluscs in life position (highest reliability); Quality 2, Mg-calcite, aragonite, travertine pipes; Quality 3, samples suspected by *Gasse and Fontes* to contain reworked material.

Lacking more complete evidence, we take the 1978 slip for each of the five sampled faults as roughly typical of past faulting events on these faults; this yields a mean repeat time of 230±135 years for the inner faults. If we adopt a less restrictive but less secure assumption and use the mean fault slip inferred for all faults reactivated in 1978 (0.34±0.16 m) as

TABLE 2. Lake Asal Highstand Elevations

| Site* | UTM-X, km | UTM-Y, km | Distance Along N36°E, km† | Elev-ation, m | S.D., m | Quality‡ |
|---|---|---|---|---|---|---|
| 1 | 226.873 | 1281.355 | -1.387 | 119.01 | 0.51 | 1 |
| 2 | 226.654 | 1281.717 | -1.352 | 120.11 | 0.51 | 1 |
| 3 | 226.281 | 1281.875 | -1.561 | 118.73 | 0.51 | 1 |
| 4 | 226.181 | 1281.406 | -1.917 | 125.76 | 0.51 | 1 |
| 5 | 227.949 | 1283.369 | 0.667 | 111.95 | 1.00 | 2 |
| 6 | 227.934 | 1283.380 | 0.661 | 102.40 | 1.00 | 2 |
| 7 | 227.914 | 1283.385 | 0.648 | 97.48 | 1.00 | 2 |
| 8 | 227.205 | 1282.562 | -0.409 | 99.90 | 1.00 | 2 |
| 9 | 227.095 | 1282.631 | -0.458 | 105.08 | 1.00 | 2 |
| 10 | 227.278 | 1282.567 | -0.347 | 100.13 | 1.00 | 1 |
| 11 | 227.367 | 1282.562 | -0.278 | 98.40 | 1.00 | 1 |
| 12 | 227.554 | 1282.623 | -0.091 | 92.33 | 1.00 | 1 |
| 13 | 227.654 | 1282.619 | -0.013 | 92.00 | 1.00 | 1 |
| 14 | 227.837 | 1282.683 | 0.173 | 93.83 | 1.00 | 1 |
| 15 | 228.020 | 1282.660 | 0.308 | 96.16 | 1.00 | 1 |
| 16 | 228.233 | 1282.709 | 0.509 | 98.50 | 1.00 | 1 |
| 17 | 227.466 | 1284.484 | 0.932 | 125.43 | 0.51 | 2 |
| 18 | 227.787 | 1284.965 | 1.474 | 132.00 | 1.00 | 3 |
| 19 | 227.679 | 1284.975 | 1.393 | 130.08 | 1.00 | 3 |
| 20 | 227.820 | 1285.072 | 1.564 | 125.94 | 1.00 | 3 |
| 21 | 227.953 | 1285.108 | 1.692 | 131.69 | 1.00 | 3 |
| 22 | 228.070 | 1285.175 | 1.826 | 130.97 | 1.00 | 3 |
| 23 | 227.223 | 1282.290 | -0.555 | 98.57 | 1.00 | 1 |
| 24 | 227.181 | 1282.270 | -0.600 | 97.94 | 1.00 | 1 |
| 25 | 226.660 | 1282.812 | -0.703 | 102.80 | 1.00 | 2 |
| 31 | 225.610 | 1281.337 | -2.420 | 122.60 | 1.41 | 3 |
| 32 | 225.621 | 1281.309 | -2.427 | 122.70 | 1.41 | 3 |
| 33 | 225.595 | 1281.251 | -2.482 | 121.10 | 1.41 | 3 |
| 34 | 225.577 | 1281.218 | -2.516 | 119.00 | 1.41 | 3 |
| 35 | 225.533 | 1281.072 | -2.638 | 128.50 | 1.02 | 1 |
| 36 | 225.506 | 1280.928 | -2.744 | 125.80 | 1.12 | 2 |
| 37 | 225.487 | 1280.955 | -2.744 | 124.60 | 1.41 | 3 |
| 38 | 225.353 | 1280.909 | -2.879 | 144.00 | 2.24 | 4 |
| 39 | 225.255 | 1280.910 | -2.958 | 136.30 | 1.41 | 3 |
| 40 | 225.925 | 1281.275 | -2.201 | 116.20 | 1.41 | 2 |
| 41 | 225.718 | 1281.348 | -2.326 | 124.00 | 1.41 | 2 |
| 42 | 225.358 | 1281.041 | -2.798 | 131.00 | 1.41 | 3 |
| 43 | 225.050 | 1280.455 | -3.391 | 130.30 | 1.41 | 3 |
| 44 | 225.202 | 1280.688 | -3.131 | 140.00 | 1.12 | 1 |
| 45 | 225.158 | 1280.848 | -3.073 | 139.50 | 1.12 | 1 |
| 51 | 228.584 | 1286.219 | 2.856 | 157.20 | 1.41 | 4 |
| 52 | 228.546 | 1286.141 | 2.779 | 157.70 | 1.41 | 4 |
| 53 | 227.974 | 1286.024 | 2.248 | 159.60 | 1.41 | 4 |
| 54 | 227.981 | 1285.895 | 2.178 | 162.50 | 1.41 | 2 |
| 56 | 228.061 | 1284.983 | 1.706 | 139.80 | 1.04 | 1 |
| 57 | 228.467 | 1285.229 | 2.179 | 131.10 | 1.41 | 4 |
| 58 | 228.284 | 1285.422 | 2.145 | 135.10 | 1.12 | 2 |
| 59 | 227.515 | 1284.617 | 1.049 | 120.30 | 1.04 | 1 |
| 60 | 227.393 | 1284.549 | 0.911 | 122.90 | 1.04 | 1 |
| 61 | 227.387 | 1284.492 | 0.872 | 132.80 | 1.41 | 4 |
| 62 | 226.349 | 1282.348 | -1.228 | 122.40 | 1.41 | 1 |
| 63 | 226.144 | 1282.103 | -1.537 | 118.50 | 1.04 | 1 |
| 64 | 226.247 | 1281.861 | -1.596 | 117.90 | 1.04 | 1 |
| 65 | 226.654 | 1281.690 | -1.368 | 116.30 | 1.04 | 1 |
| 66 | 226.756 | 1282.109 | -1.039 | 109.60 | 1.04 | 1 |
| 67 | 228.807 | 1287.247 | 3.641 | 152.30 | 1.41 | 4 |
| 68 | 228.713 | 1287.479 | 3.701 | 163.30 | 1.41 | 4 |
| 69 | 228.685 | 1287.755 | 3.840 | 154.80 | 1.41 | 4 |
| 70 | 227.622 | 1284.780 | 1.232 | 122.50 | 0.32 | 2 |
| 71 | 227.515 | 1284.661 | 1.075 | 118.15 | 0.32 | 1 |
| 72 | 227.494 | 1284.659 | 1.057 | 123.93 | 0.32 | 1 |
| 73 | 227.404 | 1284.589 | 0.943 | 120.63 | 1.00 | 3 |

the characteristic slip for all rift faults, then a repeat time of 277±116 years for all faults is obtained (Table 4).

Since about half the major faults slipped together in 1978, the recurrence time for tectonic events is likely to be less than the repeat time for individual faults. The Holocene slip on the group of faults that were reactivated in 1978 corresponds to 43% of the total Holocene fault slip (Table 4); the remaining 57% of the Holocene slip occurred on the faults that did not move in 1978. Thus the 1978 event can not be representative of all Holocene faulting in the rift. If the outer faults move together with comparable displacements, then this second group of faults has a recurrence time similar to the inner faults, and the repeat time for events somewhere in the rift should be roughly half of the ~250-year individual fault repeat time, or 125 years.

The repeat time for grouped events can be gauged independently from the ratio of the coseismic extension of the rift to the Arabia-Somalia separation rate. The amount of dike opening inferred by *Tarantola et al.* [1979, 1980] from the geodetic observations was ~2.2 m (1.5-2.9 m, Table 3); the plate separation rate across the rift during the past 1.6 m.y. is 17 mm $yr^{-1}$ [Figure 1a; *Acton et al.*, 1991]. This yields a repeat time for events on groups of faults of about 120 yr. Since a few millimeters per year of the plate separation is accommodated 10-100 km to the west of Asal (Figure 1*b*) [*Tapponnier et al.* 1990], the opening rate at the Asal rift is 15-17 mm $yr^{-1}$, and the repeat time deduced from the horizontal motion is 120-150

TABLE 2. (Continued)

| Site* | UTM-X, km | UTM-Y, km | Distance Along N36°E, km† | Elevation, m | S.D., m | Quality‡ |
|---|---|---|---|---|---|---|
| 74 | 227.548 | 1284.855 | 1.216 | 124.50 | 1.00 | 3 |
| 75 | 227.340 | 1284.617 | 0.908 | 115.36 | 5.00 | 4 |
| 76 | 227.736 | 1284.894 | 1.391 | 124.62 | 1.00 | 1 |
| 77 | 227.711 | 1284.879 | 1.362 | 125.82 | 1.00 | 3 |
| 81 | 223.782 | 1280.406 | -4.446 | 143.43 | 0.32 | 1 |
| 82 | 223.787 | 1280.386 | -4.454 | 143.09 | 0.32 | 1 |
| 83 | 223.806 | 1280.547 | -4.344 | 142.68 | 0.32 | 1 |
| 84 | 223.990 | 1280.909 | -3.982 | 135.92 | 1.00 | 1 |
| 85 | 224.110 | 1280.812 | -3.942 | 147.96 | 0.32 | 1 |
| 86 | 223.778 | 1280.697 | -4.278 | 132.46 | 1.00 | 3 |
| 87 | 225.214 | 1280.552 | -3.201 | 140.05 | 0.32 | 1 |
| 88 | 225.210 | 1280.722 | -3.105 | 139.73 | 0.32 | 1 |
| 89 | 225.168 | 1280.886 | -3.042 | 139.53 | 0.32 | 1 |
| 91 | 221.998 | 1278.616 | -6.941 | 129.18 | 1.00 | 3 |
| 92 | 222.068 | 1278.548 | -6.925 | 128.86 | 1.00 | 3 |
| 93 | 221.978 | 1278.306 | -7.140 | 130.76 | 1.00 | 2 |
| 94 | 223.336 | 1279.864 | -5.125 | 130.54 | 1.00 | 3 |
| 95 | 223.518 | 1279.887 | -4.964 | 142.98 | 0.32 | 1 |
| 96 | 223.581 | 1280.017 | -4.837 | 142.99 | 0.32 | 1 |
| 97 | 224.358 | 1278.461 | -5.123 | 146.91 | 1.00 | 2 |
| 98 | 224.199 | 1278.273 | -5.362 | 142.12 | 1.00 | 2 |
| 101 | 220.384 | 1279.873 | -7.508 | 140.62 | 1.00 | 4 |
| 102 | 220.407 | 1279.894 | -7.477 | 130.84 | 1.00 | 4 |
| 103 | 220.036 | 1279.583 | -7.960 | 129.63 | 1.00 | 2 |

* Observations carried out by *Ruegg et al.* [1990].

‡ Quality 1 is highest, 4 is lowest.

† For reference, projected distance of leveling BM 15 at UTM= (218.825, 1274.554) is -11.896 km.

TABLE 3. Fault and Dike Geometry and Moment for the 1978 Event

| Fault or Dike (see Fig. 3*b*) | Length (±25%) km | Depth (±1 km) km | Slip (±25%) m | Dip (±15°) deg | Moment* (±50%) $10^{17}$N m |
|---|---|---|---|---|---|
| Asal γ | 10.0 | 3.0 | 0.30 | 80 | 1.8 |
| Asal β | 4.0 | 1.0 | 0.10 | 60 | 0.1 |
| Asal α | 6.0 | 1.8 | 0.45 | 60 | 0.6 |
| Asal C+D | 12.0 | 1.0 | 0.35 | 60 | 1.3 |
| Asal E+F | 14.0 | 3.2 | 0.45 | 60 | 2.2 |
| Asal Dike† | 4.0 | 4.5 | 1.50 | 90 | 3.0 |
| Ghoubbet Dike† | 9.0 | 4.5 | 2.90 | 90 | 13.0 |
| *Sums:* | | | | | |
| Faults | | | | | 6.0 |
| Faults and Asal Dike | | | | | 9.0 |
| Faults and Both Dikes | | | | | 22.0 |
| $m_b$=5.3, 5.0 Earthquakes‡ | | | | | 1.7 |

* $M_o = \mu \Sigma u A$ where shear modulus μ is assumed to be 1.1 x $10^{10}$ Pa.

† Here the slip, *u*, is taken to be 70% of maximum dike opening, and length x depth is area, *A*, from *Tarantola et al.* [1890].

‡ Moment of main shocks from *Lépine et al.* [1980].

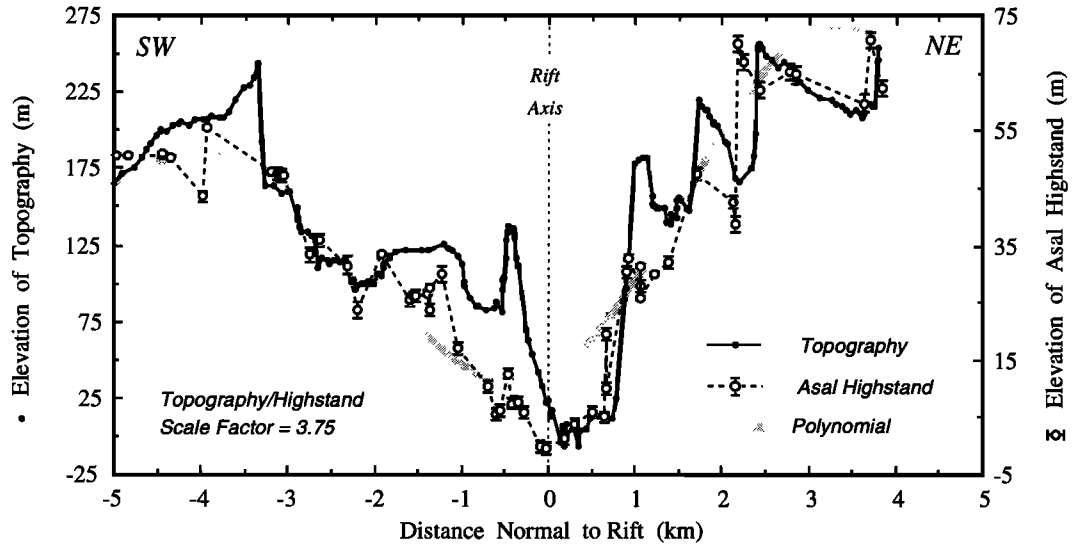


Fig. 7. Profiles of the Holocene highstand of Lake Asal and the topography, with the vertical exaggeration of the highstand 3.75 times that of the topography. The seventh-order polynomial fitted to the combined points is also shown.

years, in fair agreement with the Holocene estimate based exclusively on vertical deformation.

*Volume of Late Quaternary basalt flows.* The observation that the upper Axial Series basalt flows lie within ±2 km of the rift (Figure 2) suggests that the central rift events are accompanied by extrusion of lavas, whereas the peripheral events are purely tectonic. If seismovolcanic events recur in the central rift every 200-300 years, and each extrudes a volume of lava similar to the 10-20 x $10^6$ $m^3$ estimated for 1978 by *Allard et al.* [1979], then the basalt deposited in the rift since the topography formed is perhaps 1.0-2.5 $km^3$. The volume of the 1978 inflation we infer from *Tarantola et al.* [1979] is 27 x $10^6$ $m^3$. If distributed over the 5 x 15 km area occupied by the upper Axial Series basalts, this estimated volume yields a thickness of 15-40 m during the past 35 kyr, a value compatible with field observations.

The rate of intrusion into the rift is much lower than the volume lost to plate separation. The long term rate of dike dilatation necessary for steady state plate separation can be estimated by subjecting the combined 15-km-long and 4-km-deep dikes deduced by *Tarantola et al.* [1979] to the 16 mm $yr^{-1}$ opening rate of the rift. This yields a dilatation rate of $10^6$ $m^3$ $yr^{-1}$, which is the minimum flux rate of magma to maintain the rift shape. In 1978, the intruded volume that inflated the dike was 27 x $10^6$ $m^3$, and the volume extruded to the surface was 10-20 x $10^6$ $m^3$. Thus the maximum possible magma budget associated with the 1978 event was ~45 x $10^6$ $m^3$. Given an estimated recurrence time for such events of ~250 years, the likely flux rate comes to 0.18 x $10^6$ $m^3$ $yr^{-1}$. This flux rate is less than 20% of that needed to accommodate the rift opening purely by magma infilling, and thus the rift must subside to accommodate the loss of volume.

## DISCUSSION

### *Process of Rift Faulting*

The pattern of vertical deformation within the Asal rift demonstrates that all inner rift faults have been active during the Holocene. This means that the 1978 seismovolcanic event, in which all activity was concentrated close to the rift axis, is not the only mode of rift activity: Events distributed 2-5 km from the rift axis are just as frequent and occur on faults with dips and cumulative throws similar to those closer to the rift axis. *Rubin and Pollard* [1988] and *Rubin* [1990] showed that if faulting followed dike inflation, tensile strains imposed by the inflation could increase the tendency of normal faults located above and within a few kilometers of the dike to slip, while inhibiting slip on faults at greater depths and distances. This may be why slip in the 1978 event was restricted to shallow faults closest to the rift axis.

In general, fault slip does not diminish with distance from the rift axis (Figure 10), as *Macdonald* [1982, p. 169] proposed for slow spreading mid-ocean rifts, although faults G-K on the southwest wall do display decreasing Holocene slip or slip rate with distance from the rift (Figure 10). Outside of the rift valley, the pattern is different: Faults J, K, and probably L, located 7-8 km southwest of the rift axis, ceased during the past 8 kyr. The transition between the rift valley and its outward dipping flanks may therefore mark a mechanical transition from sustained to sporadic faulting, whereas within those boundaries, faulting is uniform. *Tapponnier and Francheteau* [1978] proposed such a transition as a boundary for plastic necking of the rift valley, and *Lin and Parmentier* [1989, 1990] used this boundary for a series of numerical experiments. At Asal, this approach appears appropriate.

The asymmetric distribution of Holocene slip in the rift may be related to the proximity of the northeast wall to the thicker crust of the Danakil horst that lies 25 km to the northeast, in contrast to the stretched basaltic rocks that extend for 100 km to the southeast (Figure 1*b*). If the crust to the southwest were thinner, a greater number of closely spaced faults might form than in the northeast.

### *Fault Depth and Geometry*

The depth of coseismic faulting and fissuring within 2 km of the rift axis is found to be remarkably shallow, <4.5 km (Figure 4*b*). *Huang and Solomon* [1987] found a 3-6 km depth (below the seafloor) and nearly pure dip-slip source mechanism (dip of 56°) for a $M_s$=5.3 shock 440 km located east of Asal on the Gulf of Aden rift. These results are quite similar to our geodetic inversion at Asal. For their study of the Mid-Atlantic Ridge, *Solomon et al.* [1988] took the thickness of the elastic lithosphere to be twice the earthquake centroid depths determined master-event relocation ($4.1 \le m_b \le 5.9$) [see *Bergman and Solomon*, 1990]. They found a thickness dependence on the spreading rate that for Asal's 8 mm $yr^{-1}$ half-spreading rate would predict the maximum depth of seismic faulting to be 10 km, three times the depth at Asal. This could mean that the elastic layer is thinner at Asal in comparison to the Mid-Atlantic Ridge. It is also possible that elastic behavior extends below the site of coseismic slip, if dike inflation precedes faulting and if compressive strains adjacent to the dike caused by its inflation are large enough to inhibit the downward propagation of slip, as proposed by *Rubin and Pollard* [1988].

The normal faults in the Asal rift dip steeply (>60°). Although the dip of faults at depth can be inferred only for the faults which slipped in 1978, evidence is seen neither for progressive rotation of fault blocks with distance from the rift axis, nor for reverse faulting on relict normal faults at or beyond the outer wall of the rift, as proposed by *Macdonald and Atwater* [1978] for mid-ocean rifts. Extreme tilting of fault blocks (>30°), which was invoked by *Verosub and Moores* [1981] to explain paleomagnetic directions along the mid-Atlantic ridge, is absent at Asal. The reactivation of groups of closely spaced normal faults leaves open the possibility that adjacent faults converge or join at shallow depth, which cannot be discerned from the geodetic or field data.

### *Similarity of Subsidence and Spreading Rates*

The Asal rift has deepened at the same rate that it has widened during the Holocene. The subsidence rate of the central rift trough is 7.8±0.9 mm $yr^{-1}$ (70 m of rift subsidence in 9±1 kyr; Figure 6), and the opening rate of the rift is 7.6±1.5 mm $yr^{-1}$ (the half-spreading rate of the Arabia-Somalia plate boundary, 8.5±1.0 mm $yr^{-1}$ [*Acton et al.*, 1991] less ~1 mm $yr^{-1}$ extension accommodated by normal faults outside of the rift). This subsidence rate is not moderated by basalt extrusion during the past 35 kyr; we infer the rate of rift infilling to be <1 mm $yr^{-1}$. If this process were to continue, the slope of the rift valley walls would approach 45° with time, regardless of its initial slope (in other words, the depth of the rift would become equal to its half-width). Instead, the rift valley walls slope ~4° (Figure 6). Taking the 11.5 km width of the rift and its ~16 mm

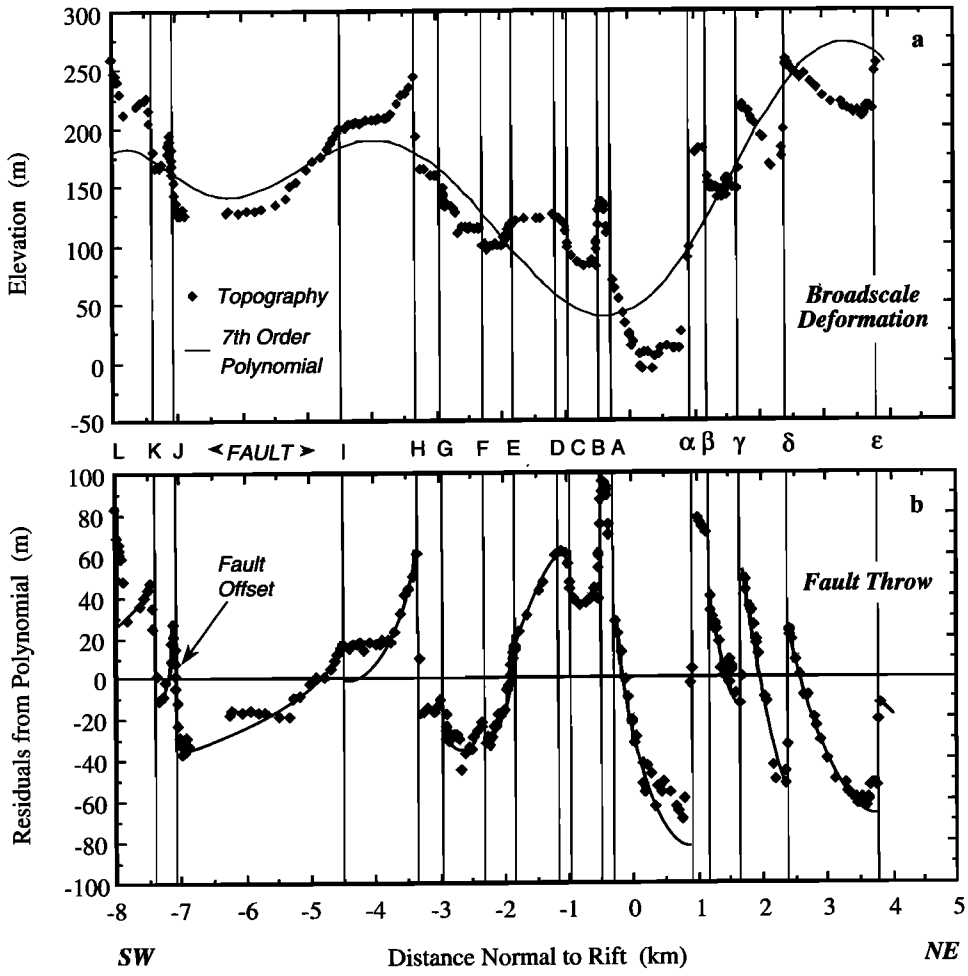


Fig. 8. (*a*) Elevation of topographic profile, with seventh-order polynomial from Figure 7. (*b*) Residual elevation from polynomial (diamonds), with interpolated structural surfaces offset by faults (curves). The surface offset at the faults is used to measure the fault throw.

$yr^{-1}$ spreading rate, the mean age of the material in the rift should be ~360 kyr. This is an order of magnitude older than the age of the formation of the topography we have inferred for the rift. Thus the long-term deformation cannot be steady state.

If the requisite faults and dikes exist to accommodate the observed 1:1 ratio opening to deepening, why isn't the rift deeper? Asthenospheric rebound, transient motion of the ductile substrate induced by the overlying fault slip, cannot account for the shallow depth of the rift, because, as shown by *King et al.* [1988], the wavelength of the rebound is much greater than the width of the rift valley: the flanks and rift axis would be uplifted by similar amounts by asthenospheric motions. Thus, even if the viscous time constant of rebound were as long as 30 kyr, the pattern of rift deformation in the rift would be little changed. We propose that the rift is kept from deepening by extrusion of voluminous basalts that periodically fill the rift valley. The most recent volcanic outpouring must predate the current topography and thus be >35 kyr. In contrast, the flux rate we infer for intrusions similar to the 1978 event is much too low to change the ratio of opening to deepening from 1:1 to the 15:1 ratio of the rift topography. Thus we suggest that the lower Axial Series basalts, which extend for 10 km normal to the rift and appear purple in Plate 1, were deposited rapidly at about 35-40 kyr.

The subaerial exposure of the Asal between the submerged sections of the rift beneath the Lake Asal and the Ghoubbet probably owes its existence to the presence of a large volcanic edifice, Fieale, that has since been fractured and distended by the nascent 35 kyr rift (Figure 2). Based on the position of fossil marine corals, Asal was submerged below sea level at 130 kyr [*Gasse and Stieltjes*, 1973]. The basalt flows and eruptive products (Figure 2) likely predate the formation of a volcanic edifice that has since uplifted the rift above sea level. While today Fieale lies at the base of the rift valley, it must once have stood as the highest point along the rift, becuase the flow directions of the lower Axial Series basalts radiate outward from Fieale (Figure 2) [*Stieltjes* , 1973, 1980].

## CONCLUSIONS

Several deductions are possible regarding the frequency of events on the rift. Repeat times for slip events on individual 5-10-km-long faults are found to be 200-300 years. Rifting episodes, such as the 1978 event, are accompanied by slip on several faults. The repeat time for events on groups of closely spaced faults is 100-150 years. Independent confirmation of the repeat time for events on groups of faults comes from the ratio of the plate separation velocity to the rift extension in 1978. We suggest that half of these events occur in the neovolcanic zone and are accompanied by basaltic eruptions; the remainder take place along the rift walls and are probably not associated with basalt flows.

There is evidence that the 1978 event at Asal is typical of undersea mid-ocean rifts. An event on the Juan de Fuca ridge,

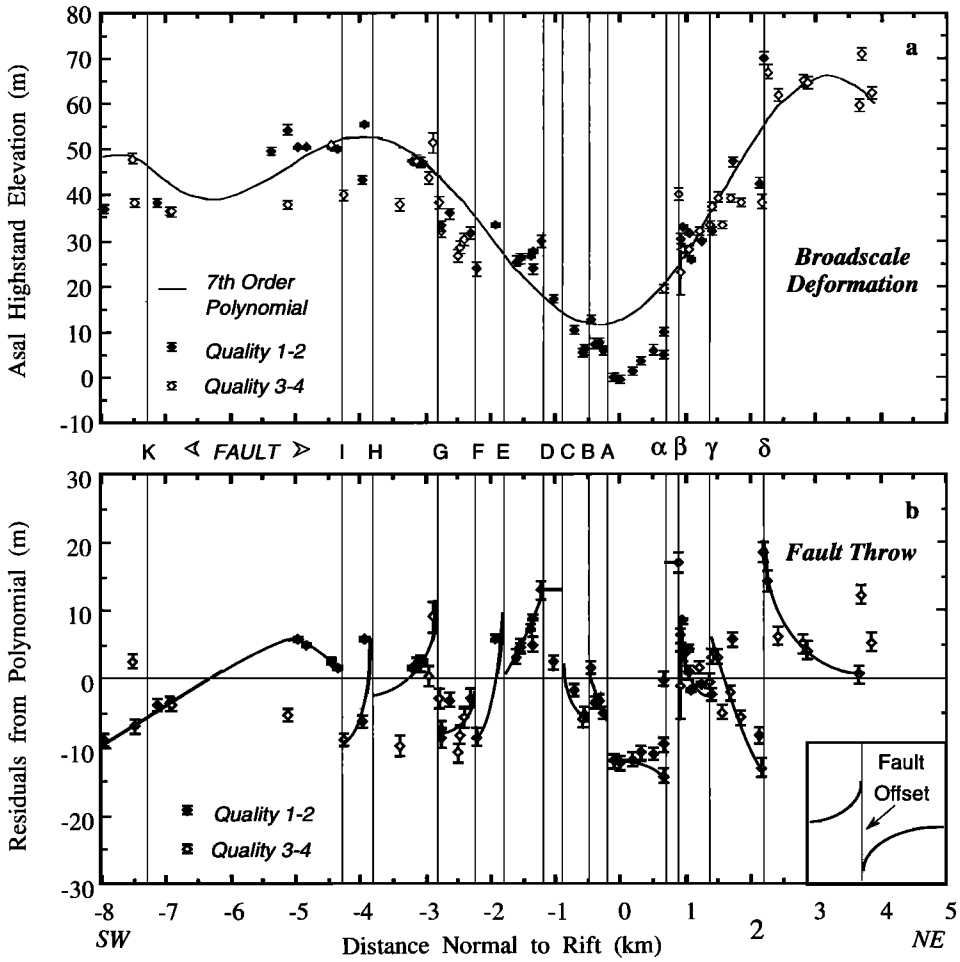


Fig. 9. (*a*) Elevation of Lake Asal highstand, with seventh-order polynomial from Figure 7. (*b*) Residual elevation from polynomial, with interpolated structural surfaces offset by faults (curves). The location of the highstand surface is guided by the higher-quality observations from *Ruegg et al.* [1990] and field observations.

TABLE 4. Fault Displacement, Fault Slip Rates, and Earthquake Repeat Times

| Inner Rift Fault | 1978 Slip at Surface,* m | 1978 Slip at Depth,† m | Holocene Slip‡ (±4 m), m | Holocene Slip Rate (±0.4 mm/yr), mm/yr | Cumulative Fault Slip (±4 m, Measured From Topography), m | Fault Age (Assumes Holocene slip rate), kyr | Late Quaternary Slip Rate (±0.3 mm/yr for 34±6 ka Fault Age), mm/yr | Holocene Repeat Time (Assumes 0.34 m Slip per Event), years |
|---|---|---|---|---|---|---|---|---|
| L | | | | | 44 | | 1.3§ | |
| J+K | | | 0.0 | 0.0 | 86 | | 2.5§ | |
| I | | | 5.6 | 0.7 | 19 | 25 | 0.5 | 461 |
| H | | | 9.1 | 1.2 | 79 | 66 | 2.3 | 284 |
| G | | | 11.9 | 1.6 | 21 | 13 | 0.6 | 217 |
| E+F | 0.1 | 0.35 | 6.3 | 0.8 | 16 | 20 | 0.5 | 410 |
| C+D | 0.4 | 0.45 | 10.5 | 1.4 | 23 | 17 | 0.7 | 246 |
| B | 0.4 | | -7.0 | -0.9 | -56 | 61 | -1.6 | 369 |
| A | 0.3 | | 7.0 | 0.9 | 67 | 73 | 1.9 | 369 |
| α | 0.3-0.4 | 0.45 | 32.0 | 4.2 | 156 | 37 | 4.5 | 81 |
| β | 0.1-0.2 | 0.10 | -13.0 | -1.7 | -56 | 33 | -1.6 | 199 |
| γ | 0.2-0.5 | 0.30 | 9.8 | 1.3 | 74 (25#) | 19 | 2.1 | 264 |
| δ | | | 32.9 | 4.3 | 81 | 19 | 2.3 | 79 |
| ε | | | | ? | 63 | | 1.8§ | |
| Mean | 0.3±0.1 | 0.34±0.16 | | | | 35±22 | | 277±116** |

Blank entries indicate fault not sampled; rift-side-down slip reckoned positive.

* Slip measured at the surface by *Abdallah et al.* [1979] and *Le Dain et al.* [1979] along their cross sections 2 and 3.

† Inverted from leveling data.

‡ 43% of the Holocene slip (or slip rate, as portrayed in column) occurred on faults that were active in 1978.

§ Outermost faults may predate inner faults, so 35 ka assumed age may be invalid.

# Cumulative fault slip corrected for misalignment of shoreline and topographic profile.

** Mean for faults which slipped in 1978; mean is 230±135 years if 1978 slip on each fault is used.

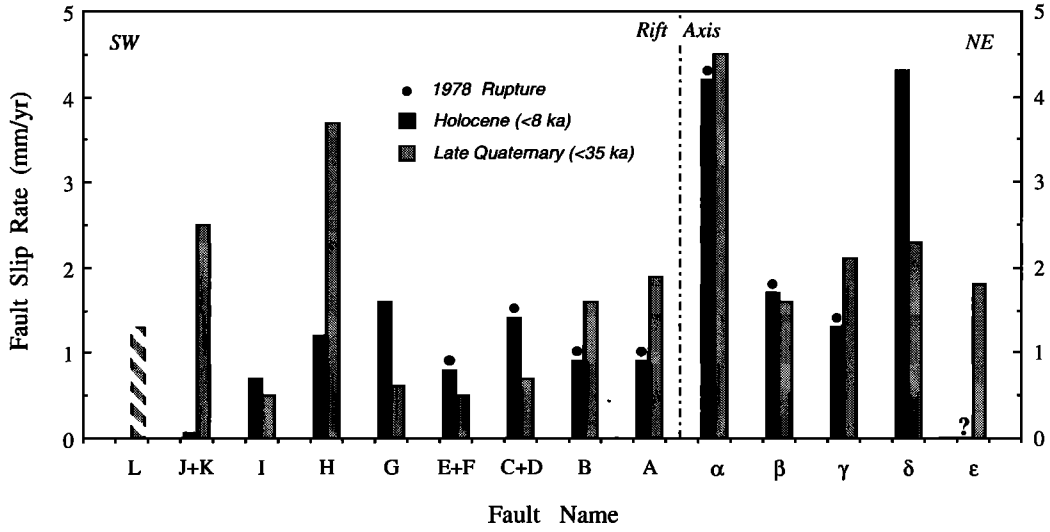


Fig. 10. Measured Holocene and inferred late Quaternary slip rates for the sampled faults in the Asal rift (from Table 4). Faults that slipped at the surface in 1978 are highlighted.

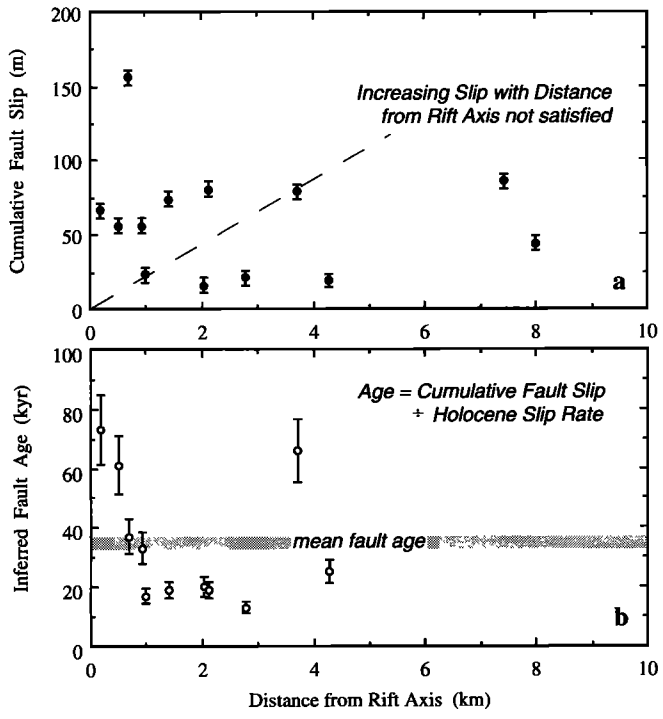


Fig 11. (*a*) Cumulative displacement on the rift faults and (*b*) their inferred age as a function of distance. Note that fault throw does not increase with distance from the rift axis (dashed line).

which occurred between 1981 and 1987, extends for 15 km and deposited ~50 x $10^6$ $m^3$ of basalt [*Chadwick et al.*, 1991]; the 1978 Asal event was 10-20 km long and deposited at least 10-20 x $10^6$ $m^3$ of basalt. If the repeat behavior at Asal characterizes the Mid-Atlantic (10-35 mm $yr^{-1}$ half-spreading rate) or Juan de Fuca (30 mm $yr^{-1}$) ridges, then detection of a tectonic event during a 5-year-long program would require monitoring of 200-300 km of rift; to capture a volcanic event, 400-600 km of rift would need to be monitored with geodetic instruments spaced roughly every 5 km along the rift, a formidable task. Such a spacing is necessary to assure observations of 10-15-km-long ridge events on at least two instruments. Given the largely aseismic nature of the Asal rift event and plate separation along the mid-Atlantic ridge, large-scale deployment of ocean bottom tiltmeter-seismometer devices [such as those developed by *Staudigel et al.*, 1991] for geodetic measurement of seafloor deformation would be essential for event detection on slow spreading ridges.

The mechanics of rifting at Asal is dominated by steeply dipping dikes and faults. The 1978 deformation associated with the seismovolcanic event at Asal was largely aseismic (<30% of the moment was released at seismic periods) and shallow (2-4 km deep). All inner rift faults were similarly active during the past 8 kyr, and also during the past 35-kyr interval. Little or no progressive rotation of fault blocks is seen as the faults are carried farther from the rift axis. Rather, faults continue to slip until they approach the edges of the inner rift, at which point slip diminishes, becomes sporadic or ceases.

The striking similarity of the Holocene deformation represented by the highstand and the long-term deformation preserved by the topography means that the process of rifting has been steady state, and largely devoid of volcanism, during the past 30-40 kyr. But the fact that the inferred age of the topography is so young in comparison to the 0.5-1.0 Ma age of rifting means that the process of rifting could not have been steady state before 30-40 kyr. The rapid subsidence that characterizes the past 30 kyr succeeded a period of volcanism that largely filled the rift. It seems unlikely that the horizontal motions within the rift valley could be steady for periods much longer than 30 kyr given the dramatic changes in the vertical motions. We lack precise geologic markers, however, that would enable us to measure the 30- to 100-kyr changes in plate separation within the rift.

The Holocene subsidence rate at the Asal rift is equal to the half-spreading rate. The basalt deposition rate during the past 30 kyr has been much less than the subsidence rate of 8 mm $yr^{-1}$, and so does little to modify the similarity between the subsidence and half-spreading rates. Thus rift growth has been self-similar since 35 kyr. If growth were self-similar over much longer time periods, the 7.5-km-wide inner rift would be 3.5 km deep rather than the observed 300 m. This suggests that voluminous extrusive episodes periodically fill in the rift. The last such event may have occurred ~35 kyr; additional dates on the basalt flows are needed to test the hypothesis of widespread extrusion at that time, and to see if past episodes of

basaltic extrusion are cyclic. *Patriat and Courtillot* [1984] and *Courtillot et al.* [1984] proposed a 1-m.y.-long cycle of alternating effusive and tectonic modes of rifting along propagating rifts such as Asal.

The similarity of subsidence and half-spreading rates, combined with the low Holocene basalt flux rate we infer at Asal, impose a strong constraint on the mechanics of rift growth. Whereas the site of volcanism might be stable, these observations require that rifting evolution is not steady state, but instead has cycled at least once from volcanism to downwarping. Is such a cycle present along other slow spreading rifts and does it repeat? *Chen and Morgan* [1990*a*, *b*] show that mid-ocean rift growth may indeed be steady state under some boundary conditions, so whether the cycling we infer for Asal is exceptional or typical for undersea rifts is unknown. The variation of topography along the Mid-Atlantic rift axis, with the likelihood that focused magmatic accretion occurs at any one time only at isolated locations [*Lin et al.*, 1990; *Phipps Morgan*, 1991], suggests that rifting is not steady state, although it is difficult to infer a time constant from these observations.

The Asal highstand furnishes an invaluable tool for deciphering the rifting process at Asal; it is unlikely that any such record will ever be available on mid-ocean rifts. We are fortunate that the Lake Asal highstand is located at nearly the same position as the leveling line, enabling direct comparison of contemporary and Holocene vertical deformation. Without the Holocene record, one might have surmised that the 1978 event, with fault slip restricted to the rift axis, typifies rift events. To explain the large cumulative slip on faults farther from the rift evident from the topography, one would have concluded that faults become progressively inactive with increasing distance from the rift, an erroneous deduction. On the contrary, if we had the Holocene record but lacked the 1978 event deformation, it would not have been possible to infer repeat times from the Holocene fault slip rates. Finally, without the horizontal geodetic observations of the 1978 event, we would not have been able to corroborate our estimate of the repeat time for seismovolcanic events on the rift.

*Acknowledgements.* This work grew out of a field trip to Djibouti in 1989, while R.S. was a Visiting Professor at Laboratoire de Tectonique, Institut de Physique du Globe, Paris. R.S. is grateful for financial support offered by IPGP and Université de Paris VII, during his stays in 1989 and 1991, and to Albert Tarantola, who furnished additional funds in 1990. Financial support for the field trip was provided by Observatoires de Géophysique, IPGP, and by Programme AFAR of "Dynamique et Bilan de la Terre", INSU, Paris. We are also grateful for the logistical support offered by the Observatoire Géophysique d'Arta and the Institut Supérieur d'Etude et de Recherche Scientifique, Djibouti. We greatly appreciated the insights of Rolando Armijo in the field and lab. For their contribution to the field work, we thank Isabelle Manighetti, Denis Hatzfeld, Gilles Lambaré, Jean Bernard de Chabalier, Thierry Duquesnoy, and Pierre-Yves Gillot. Finally, we would like to thank Gary Acton, Richard Gordon, Jian Lin, Thomas Brocher, Carl Mortenson, Janet Morton, and Allan Rubin for thoughtful reviews of the manuscript.

## REFERENCES

Abdallah, A., V. Courtillot, M. Kasser, A.-Y. Le Dain, J.-C. Lépine, B. Robineau, J.-C. Ruegg, P. Tapponnier, and A. Tarantola, Relevance of Afar seismicity and volcanism to the mechanics of accreting plate boundaries, *Nature*, *282*, 17-23, 1979.

Acton, G.D., S. Stein, and J.F. Engeln, Block rotation and continental extension: A microplate model for Afar, *Tectonics*, *10*, 501-526, 1991.

Allard, P., H. Tazieff, and D. Dajlevic, Observations of seafloor spreading in Afar during the November 1978 eruption, *Nature*, *279*, 30-33, 1979.

Barberi, F., and J. Varet, Volcanism of Afar: Small-scale plate tectonics implications, *Geol. Soc. Am. Bull.*, *88*, 1251-1266, 1977.

Bergman, E.A., and S.C. Solomon, Earthquake swarms on the Mid-Atlantic Ridge: Products of magmatism or extensional tectonics?, *J. Geophys. Res.*, *95*, 4943-4966, 1990.

Chadwick, W. W., Jr, R. W. Embley, and C. G. Fox, Evidence for volcanic eruption on the southern Juan de Fuca Ridge between 1981 and 1987, *Nature*, *350*, 416-418, 1991.

Chase, C. G., Plate kinematics: The Americas, East Africa, and the rest of the world, *Earth Planet. Sci. Lett.*, *37*, 355-368, 1978

Chen, Y., and W. J. Morgan, Rift/no rift transition at mid-ocean ridges, *J. Geophys. Res.*, *95*, 17,571-17,581, 1990*a*.

Chen, Y., and W. J. Morgan, A nonlinear rheology model for mid-ocean ridge axis topography, *J. Geophys. Res.*, *95*, 17,583-17,604, 1990*b*.

Courtillot, V., Propagating rifts and continental breakup, *Tectonics*, *1*, 239-250, 1982.

Courtillot, V., A. Galdeano, and J.L. LeMouel, Propagation of an accreting plate boundary: A discussion of new aeromagnetic data in the Gulf of Tadjurah and southern Afar, *Earth. Planet. Sci. Lett.*, *47*, 144-160, 1980.

Courtillot, V., J. Achache, F. Landre, N. Bonhommet, R. Montigny, and G. Féraud, Episodic spreading and rift propagation: New paleomagnetic and geochronologic data from the Afar nascent passive margin, *J. Geophys. Res.*, *89*, 3315-3333, 1984.

Courtillot, V., R. Armijo, and P. Tapponnier, Kinematics of the Sinai triple junction and a two-phase model of Arabia-Africa rifting, in Continental Extensional Tectonics, edited by M.P Coward, J.F. Dewey, and P.L. Hancock, *Spec. Publ. Geol. Soc. Am. 28*, 559-573, 1987.

DeMets, C., R.G. Gordon, D.F. Argus, and S. Stein, Current plate motions, *Geophys. J. Int.*, *101*, 425-478, 1990.

Gasse, F., Sedimentary formations in northern and southern Afar, in *Geology of Central and Southern Afar (Ethiopia and Djibouti Republic)*, edited by J. Varet, 1:500,000 scale map and 124 pp. report, pp. 37-68, Editions du Centre National de la Recherce Scientifique, Paris, 1978.

Gasse, F., Tectonic and climatic controls on lake distribution and environments in Afar from Miocene to present, Lacustrine Basin Exploration: Case Studies and Modern Analogs, Edited by B. Katz, AAPG *Mem. 50*, 19-41, 1991.

Gasse, F., and J.-C. Fontes, Paleoenvironments and paleohydrology of a tropical closed lake (Lake Asal, Djibouti) since 10,000 yr B.P., *Paleogeography, Paleoclimatology, Paleoecology*, *69*, 67-102, 1989.

Gasse, F., and M. Fournier, Plio-Quaternary deposits and tectonics of the margins of the Gulf of Tadjura (Republic of Djibouti), *Bull. Cent. Rech. Explor. Prod., Elf-Aquitaine*, *7*, 285-3000, 1983.

Gasse, F., and L. Stieltjes, Les sédiments du quaternaire récents du lac Asal (Afar central, territoire française des Afars et des Issas), *Bull. Bur. Rech. Géol. Mini., Sect. 4*, 4, 229-251, 1973.

Gaulier, J.-M., and P. Huchon, Tectonic evolution of Afar triple junction, *Bull. Soc. Géol. Fr., 162* , 451-464, 1991.

Hauksson, E., Episodic rifting and volcanism at Krafla in North Iceland: Growth of large ground fissures along the plate boundary, *J. Geophys. Res.*, *88*, 625-636, 1983.

Huang, P. Y., and S. C. Solomon, Centroid depths and mechanisms of mid-ocean ridge earthquakes in the Indian ocean, Gulf of Aden, and Red Sea, *J. Geophys. Res.*, *92*, 1361-1382, 1987.

Institut Géographique National de France, Implantation d'un réseau géodésique pour la mesure directe de l'expansion d'un rift océanique, *RCP 180, 9th ed.*, 91 pp., Saint Mandé, 1975.

King, G.C.P., R.S. Stein, and J.B. Rundle, The growth of geological structures by repeated earthquakes, 1, Conceptual framework, *J. Geophys. Res.*, *93*, 13,307-13,318, 1988.

Le Dain, A.-Y., B. Robineau, and P. Tapponnier, Les effets tectoniques de l'événment sismique et volcanique de novembre 1978 dans le rift d'Asal-Ghoubbet, *Bull. Soc. Géol. France, 22*, 817-822, 1979.

Lépine, J.C., J.-C. Ruegg, and A.M. Abdallah, Sismicité du rift d'Asal-Ghoubbet pendant la crise sismo-volcanique de novembre 1978, *Bull. Soc. Géol. Fr., 22*, 809-816, 1980.

Lin, J., and E.M. Parmentier, Mechanisms of lithospheric extension at mid-ocean ridges, *Geophys. J. R. Astron. Soc.*, *96*, 1-22, 1989.

Lin, J., and E.M. Parmentier, A finite amplitude necking model of rifting in brittle lithosphere, *J. Geophys. Res.*, *95*, 4909-4924, 1990.

Lin, J., G.M. Purdy, H. Schouten, J.-C. Sempéré and C. Zervas, Evidence from gravity data for focused magmatic accretion along the mid-Atlantic ridge, *Nature, 344*, 627-632, 1990.

Macdonald, K.C., Mid-ocean ridges: Fine scale tectonic, volcanic and hydrothermal processes within the plate boundary zone, *Annu. Rev. Earth Planet. Sci., 10*, 155-190, 1982.

Macdonald, K.C., and T.M. Atwater, Evolution of rifted ocean ridges, *Earth Planet Sci. Lett., 39*, 319-327, 1978.

Morton, W.H., and R. Black, Crustal attenuation in Afar, in Afar Depression of Ethiopia, edited by A. Pilger and A. Rösler, *Sci. Rep. 14*, pp. 55-65, Inter-Union Committee on GeodynamicsStuttgart, 1975.

Okyada, Y., Surface deformation due to shear and tensile faults in a half space, *Bull. Seismol. Soc. Am., 75*, 1135-1154, 1985.

Patriat, P., and V. Courtillot, On the stability of triple junctions and its relation to episodicity in spreading, *Tectonics, 3*, 317-332, 1984.

Pham Van Ngoc, D. Boyer, J.-L. Le Mouël, and V. Courtillot, Propriétés électriques de la croûte et du manteau supérieur du rift d'Asal (Djibouti) d'après les sondages magnéto-telluriques profonds, *Bull. Soc. Géol. Fr., 22*, 863-871, 1980.

Phipps Morgan, J., Mid-ocean ridge dynamics: Observations and theory, U.S. Nat. Rep. Int. Un. Geod. Geophys. 1987-1990, *Rev. Geophys., Supplement*, 807-822, 1991.

Richard, O., Etude de la transition dorsale océanique-rift émergé: Le Golfe de Tadjoura (République de Djibouti), thèse 3è cycle, Univ. de Paris-Sud, Orsay, 1979.

Rubin, A.M., A comparison of rift-zone tectonics in Iceland and Hawaii, *Bull. Volcanol., 52*, 302-319, 1990.

Rubin, A.M., and D.D. Pollard, Dike-induced faulting in rift zones of Iceland and Afar, *Geology, 16*, 413-417, 1988.

Ruegg, J.-C., J.C. Lépine, A. Tarantola, and M. Kasser, Geodetic measurements of rifting associated with a seismovolcanic crisis in Afar, *Geophys. Res. Lett., 6*, 817-820, 1979.

Ruegg, J.-C., J.C. Lépine, and C. Vincent, Sismicité et microsismicité de la dorsale de Tadjoura, tectonique et frontière de plaques, *Bull. Soc. Géol. Fr., 22*, 917-923, 1980.

Ruegg, J.-C., A. Tarantola, M. Kasser, J.C. Lépine, and J.J. Leveque, Mouvements actuels de déformation dans le rift d'Asal (Djibouti): Réajustement post-sismique ou nouvelle phase d'étirement tectonique?, *Ann. Géophys., 38*, 391-403, 1982.

Ruegg, J.-C., Main results about the crustal and upper mantle structure of the Djibouti region (T.F.A.I.), in *Afar Depression of Ethiopia*, A. Pilger and A. Rösler, Eds., Inter-Union Comm. on Geodynam., Sci. Rep. 14, p. 120-134, Stuttgart, 1975.

Ruegg, J.-C., and M. Kasser, Deformation across the Asal-Ghoubbet rift, Djibouti, uplift and crustal extension 1979-1986, *Geophys. Res. Lett., 14*, 745-748 1987.

Ruegg, J.-C., M. Kasser, and J.C. Lépine, Strain accumulation across the Asal-Ghoubbet rift, Djibouti, East Africa, *J. Geophys. Res., 89*, 6237-6246, 1984.

Ruegg, J.-C., F. Gasse, and P. Briole, Mouvements du sol holocènes dans rift d'Asal à Djibouti, *C.R. Acad. Sci., 310*, 1687-1694, 1990.

Sempéré, J.-C., and K.C. Macdonald, Marine Tectonics: Processes at mid-ocean ridges, *Rev. Geophys., 25*, 1313-1347, 1987.

Solomon, S.C., P.Y. Huang, and L. Meinke, The seismic moment budget of slowly spreading ridges, *Nature, 334*, 58-60, 1988.

Staudigel, H., F.K. Wyatt, and J. O. Orcutt, Ocean bottom tiltmeter developed for submarine volcano monitoring, *EOS, Trans. AGU, 72*, 289-295, 1991.

Stieltjes, L., L'axe tectono-volcanique d'Asal (Afar central, territoire Française des Afar et des Issas), thèse de 3e cycle, Univ. de Paris-Sud, Orsay, 1973.

Stieltjes, L., *Carte Géologique du Rift D'Asal, République de Djibouti (Dépression Afar, Est-Africain)*, Scale 1:50000, Centre National de la Recherche Scientifique, Paris, 1980.

Tapponnier, P., and J. Francheteau, Necking of the lithosphere and the mechanics of slowly accreting plate boundaries, *J. Geophys. Res., 83*, 3955-3970, 1978.

Tapponnier, P., and J. Varet, La zone de Mak'Arassou en Afar: un équivalent émergé de "failles transformantes" océaniques, *C. R. Acad. Sci., Ser. D, 278* , 209-212, 1974.

Tapponnier, P., R. Armijo, I. Manighetti, and V. Courtillot, Bookshelf faulting and horizontal block rotations between overlapping rifts in southern Afar, *Geophys. Res. Lett., 17*, 1-4, 1990.

Tarantola, J.C. Ruegg, and J.C. Lépine, Geodetic evidence for rifting in Afar: A brittle-elastic model of the behavior of the lithosphere, *Earth Planet. Sci. Lett., 45*, 435-444, 1979.

Tarantola, J.C. Ruegg, and J.P. Lépine, Geodetic evidence for rifting in Afar, 2. Vertical displacements, *Earth Planet. Sci. Lett., 48*, 363-370, 1980.

Tucholke, B.E., K.C. Macdonald, and P.J. Fox, ONR seafloor natural laboratories on slow- and fast-spreading mid-ocean ridges, *Eos Trans. AGU, 72*, 268-270, 1991.

Varet, J., *Geology of Central and Southern Afar (Ethiopia and Djibouti Republic)*, scale 1:500,000 map and 124 pp. report, Editions du Centre National de la Recherce Scientifique, Paris, 1978.

Vellutini, P., The Manda-Inakir rift, Republic of Djibouti: A comparison with the Asal rift and its geodynamic interpretation, *Tectonophysics, 172*, 141-153, 1990.

Vening Meinesz, F.A., Les "graben" africans résultat de compression ou de tension dans la croûte terrestre?, *Inst. R. Colon. Belge Bull. Seances, 21*, 539-552, 1950.

Verosub, K.L., and E.M. Moores, Tectonic rotations in extensional regimes and their paleomagnetic consequences for oceanic basalts, *J. Geophys. Res., 86*, 6335-6350, 1981.

P. Briole, J.-C. Ruegg, and P. Tapponnier, Institut de Physique de Globe de Paris, 4, Place Jussieu, 75252 Paris Cedex 05, France; Fax 33 1 44 27 33 73.

F. Gasse, Laboratoire d'Hydrologie et de Géochimie isotopique, Bât. 504, Université de Paris-Sud, 91405 Orsay Cedex, France; Fax 33 1 64 46 59 38.

R.S. Stein, U.S. Geological Survey, 345 Middlefield Road, MS 977, Menlo Park, CA 94025; Tel 415-329-4840; Fax 415 329 5163.

(Received May 2, 1991;
revised July 29, 1991;
accepted August 12, 1991.)